Monosaccharide-Responsive Polymers of Boronic acid Derivatives and Their Medical Applications

Hyunkyu Kim

Graduate Program of Chemistry

Ulsan National Institute of Science and Technology (UNIST)

Monosaccharide-Responsive Polymers of Boronic acid Derivatives and Their Medical Applications

A thesis

Submitted to the Graduate School of UNIST

In partial fulfillment of the

Requirements for the degree of

Master of Science

Hyunkyu Kim

1. 28 2013 Month/Day/Year of submission

Approved by

_____

Major Advisor

Kyoung Taek Kim

Monosaccharide-Responsive Polymers of Boronic acid Derivatives and Their Medical Applications

Hyunkyu Kim

This certifies that the thesis of Hyunkyu Kim is approved.

1. 28. 2013 Month/Day/Year of submission

signature

_____

Kyoung Taek Kim

signature

_____

Sung You Hong

signature

_____

Ja-Hyoung Ryu

Abstract

Monosaccharide-Responsive Polymers of Boronic acid Derivatives and Their Medical Applications, 2013, Hyunkyu Kim, Graduate Program of Chemistry, Ulsan National Institute of Science and Technology (UNIST).

Boroxole-containing styrenic monomer was synthesized from 3-bromo-4-(bromomethyl)benzonitrile in seven steps and block copolymers of Poly(styreneboroxole) (PBOx) and poly(ethylene glycol) (PEG) were synthesized by the reversible addition−fragmentation and chain transfer (RAFT) method. The resulting amphiphilic block copolymer, PBOx-*b*-PEG, displayed binding to monosaccharides in phosphate buffer at neutral pH, as quantified by Wang's competitive binding experiments. These block copolymers self-assembled into a variety of nanostructures including spherical and cylindrical micelles and polymer vesicles in water according to degree of polymerization of the PBOx block. The morphology of the self-assembled structures were observed on transmission electron microscopy (TEM) and dynamic light scattering (DLS),

Polymersomes of these block copolymers exhibited monosaccharide-responsive disassembly in a neutral-pH medium. Disassembly of polymersomes was studied by UV-Vis spectrophotometer and DLS. These polymersomes stored fluorescein isothiocyanate (FITC)-labeled human insulin (F-insulin) within the water-filled inner compartment. Encapsulation of F-insulin within polymersomes was confirmed by laser confocal fluorescence microscopy (LCFM). Encapsulated insulin could be released from the polymersomes only in the presence of sugars under physiological pH conditions. The result was verified by fluorescence intensity.

Sequence-specific copolymer of styreneboroxole and N-functionalized maleimide was synthesized by RAFT polymerization method in the presence of a poly(ethylene glycol)-chain transfer agent. These polymers have a glucose receptor alternating with a nonresponsive solubilizing group throughout the sugar-responsive epolymer chain. This new system promotes further diffusion of glucose to bilayer membrane and essentially induces disassembly of the membrane into individual block polymers so these polymersomes become more sensitive to lower glucose concentrations than PBOx-*b*-PEG. It shows low cytotoxicity, serum compatibility, and sugar-responsive behavior at a glucose level close to physiologically relevant conditions that prove promising for controlled delivery applications for glucose-related diseases such as diabetes.

Contents

List of Tables

List of Schemes

List of Figures

List of Abbreviation

AIBN	Azobisisobutyronitrile
ARS	Alizarin Red S
ATRP	Atom transfer radical polymerization
n-BuLi	n-Butyllithium
CTA	Chain transfer agent
DIBAL-H	Diisobutylaluminium hydride
DLS	Dynamic light scattering
DMF	*N,N'*-dimethylformamide
DP_n	Number average degree of polymerization
F-insulin	Fluorescein isothiocyanate (FITC)-labeled human insulin
FITC	Fluorescein isothiocyanate
FT-IR	Fourier-transform infra red spectroscopy
GPC	Gel permeation chromatography
LCFM	Laser confocal fluorescence microscopy
MALDI−TOF	Matrix-assisted laser desorption/ionization-Time of flight
M_n	Number average molecular weight
MOM	Methoxymethyl
MW	Molecular weight
NMR	Nuclear magnetic resonace
O.T	Optical transmittance
PBA	Phenylboronic acid
PDI	Polydispersity index
PEG	Poly(ethylene glycol)
PBOx	Poly(styreneboroxole)
PS	Polystyrene
RAFT	Reversible addition-fragmentation chain transfer
TBDMS	tert-butyldimethylsilyl
THF	Tetrahydrofuran
TEM	Transmission electron microscopy
TLC	Thin-layer chromatography

Chapter 1. Introduction

1.1 Glucose-responsive polymer

Many important substances in living systems respond to external stimuli and adapt themselves to changing conditions. Polymer scientists have been trying to mimic these behaviors and the interest of stimuli-responsive polymers has become increasingly for many decades. These polymers alter their physical and chemical properties in response to the external stimuli, so these polymers can be regulated in correspondence to the external stimuli, such as temperature, pH, light, and the presence of stimulant molecules[1,2]. Among stimuli-responsive polymers, the polymers that respond to glucose have considerable attention due to their promising application in both insulin delivery system and glucose sensing[3]. Not only diabetes is a chronic disease, but also the number of diabetics continues to increase. The most widely used method to control the blood sugar level is direct insulin injection and monitor the blood sugar level regularly. Two things give patients dangerousness and low compliance. One potential solution to solve the problems is the development of smart delivery system which regulates the blood sugar level automatically, so noticeable researches are are go along going along nicely to develop the self-regulated insulin delivery system based on glucose-responsive polymers.

1.2 Boronic acid

The organic molecules including B atoms are used in carbon-carbon bond formation reactions through transition-metal-catalyzed coupling so they are vital in developing the new organic materials with optical or electronic properties[4]. The organoboronic acid has form of aromatic compounds containing boron atoms and typically acts as a Lewis acid due to the presence of the empty p orbital of the boron atom. In 1954, Kuivila found phenylboronic acid forms boronate ester with 1, 2- or 1, 3-diol compound such as monosaccharide[5] (Figure 1.1).

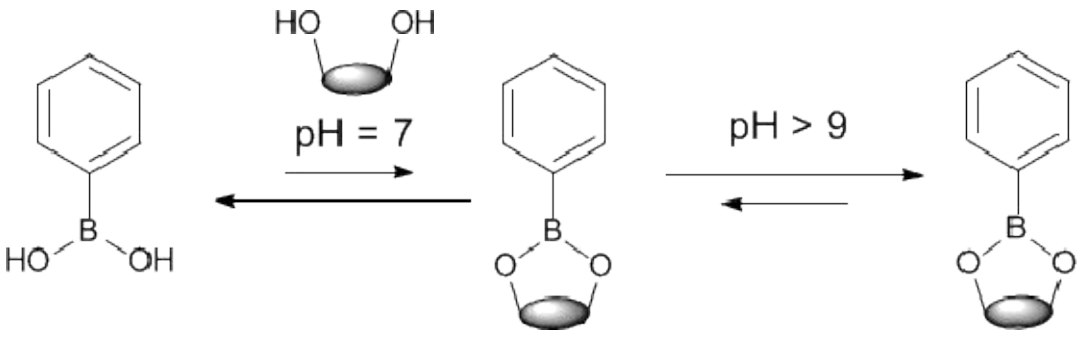

Figure 1.1 Diol complexation equilibria of Phenylboronic acids (PBS) in aqueous Solution.

However, the form of boronate ester is in equilibrium and at neutral pH aqueous condition, hydrolysis of boronate esters is favored because of angle strain (120° → 108°). Therefore, through ionization boronate ester can be become to sp^3 hybrid orbital and be stabilized in high pH condition (>9)[6] (Figure 1.1). These phenomena of organoboronic acids are available for the recognition of monosaccharide molecules in the aqueous solution. Therefore, it can be used as glucose sensor or insulin delivery materials so the development of polymeric materials with these properties has attracted a lot of attention in recent years.

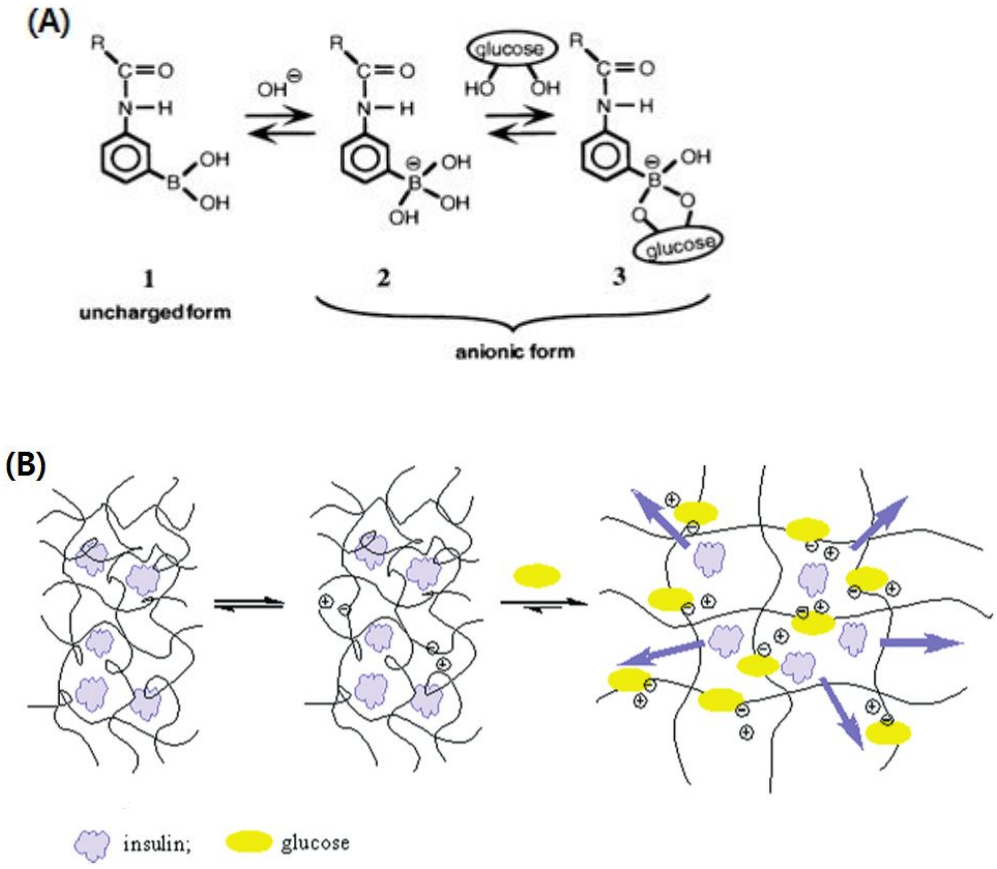

Figure 1.2 (A) Equilibria of (Alkylamido)phenyl boronic acid (B) Schematic illustration of glucose-triggered swelling of hydrogel and release of FITC-insulin from the hydrogel at 28 °C, pH 9.0[7].

Kataoka introduced monosaccharide cognitive function of organoboronic acid into polymer materials and pursued an investigationof it on the glucose sensor and insulin releasing materials for the first time[7]. He adopted phenyboronic acid at cross-linked acrylic acid polymer and synthesized hydrogels having a function of monosaccharide recognition (Figure 1.2 (a)). Phenylboronic acid

(PBA) in the cross-linked hydrogel binds to monosaccharides and then becomes ionized so the gel is swelled. At this time, encapsulated insulin in the gel is discharged to the outside by diffusion (Figure 1.2 (b)). This first attempt proved that monosaccharide-responsive polymers can be synthesized through a way to change the physical properties of polymers and these hydrogels containing boronic acid can be used as the self-regulating insulin delivery materials.

However, Boronate ester dominantly hydrolyze in aqueous solutions at neutral pH, so boronic acid-containing polymers have been mainly used under high pH conditions (>9) that are incompatible for the use of these polymers under physiological conditions.

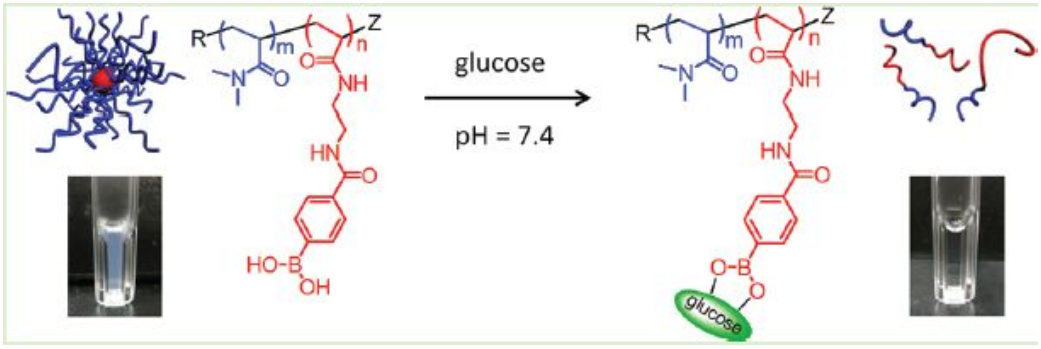

Figure 1.3 A schematic representation of glucose-triggered disassembly of micelles of sugar-responsive block copolymers[8].

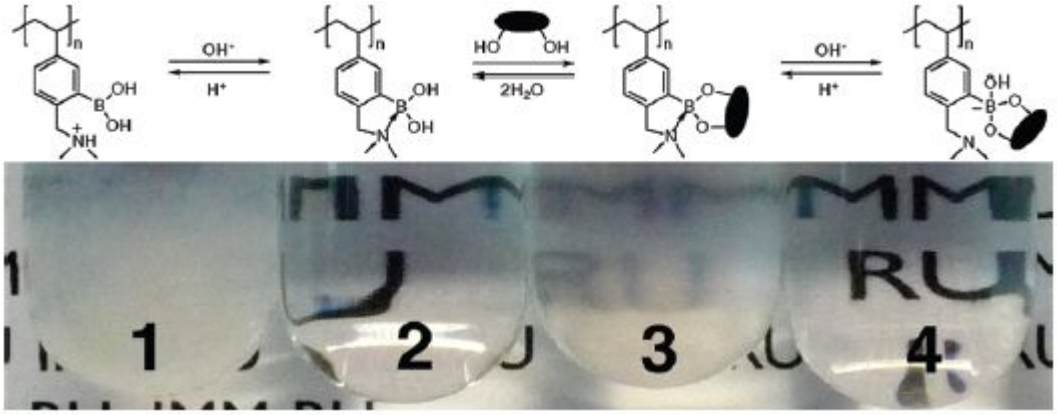

Figure 1.4 A schematic representation of the polymer with monosaccharides in different pH environments. The photograph shows tubes containing the polymer in different buffers after 18 h. Tube **1**: **7** in PBS (pH) 7.4), **2**: in PBS/D-fructose (50 mM), **3**: in PBS/D-glucose (100 mM), **4**: in TRIS/ D-glucose (100 mM, pH) 7.8)[10].

The problem can be solved when boronate esters are stabilized in neutral aqueous solution by decreasing the pK_a of the PBA. The introduction of strongly electron-withdrawing substituents such as NO_2, halogen, amide to the phenylboronic acid on meta and para position[8-10] (Figure 1.3) and the introduction of an intramolecular electron sharing substituents such as dialkylaminomethyl, hydroxymethyl to phenylboronic acid on ortho position[11,12] (Figure 1.4) can decrease the pK_a of PBA so these methods make it possible to use boronic acid containing polymers under physiological conditions. Therefore, these materials have potentials in the areas of saccharide sensing and self-regulating insulin delivery applications

1.3 Well- Defined Copolymer

To apply the unique properties of boronic acid-containing polymers efficiently to sensing or drug delivery system, it is important to synthesize well-defined copolymers with reliable molecular weights and narrow molecular weight distributions. Controlled radical polymerization is a synthetic method which controls these aspects. Atom transfer radical polymerization (ATRP)[13-15] and Reversible addition-fragmentation chain transfer (RAFT)[16-20] polymerization have been used to synthesize the well-defined boronic acid-containing polymers. Firstly, Jäkle et al. reported the efficient synthesis of monosaccharide responsive polymers using ATRP from the polymerization of organoboron monomers or silylated precursors[21] (Sheme 1.1). Summerlin et al. employed RAFT polymerization and synthesized amphiphilic block copolymers firstly which can be self-assembled to micelles[22] (Scheme 1.2). However, because these polymers have the the pinacol ester, they need deprotection to have boronic acid-containing polymers after polymerization.

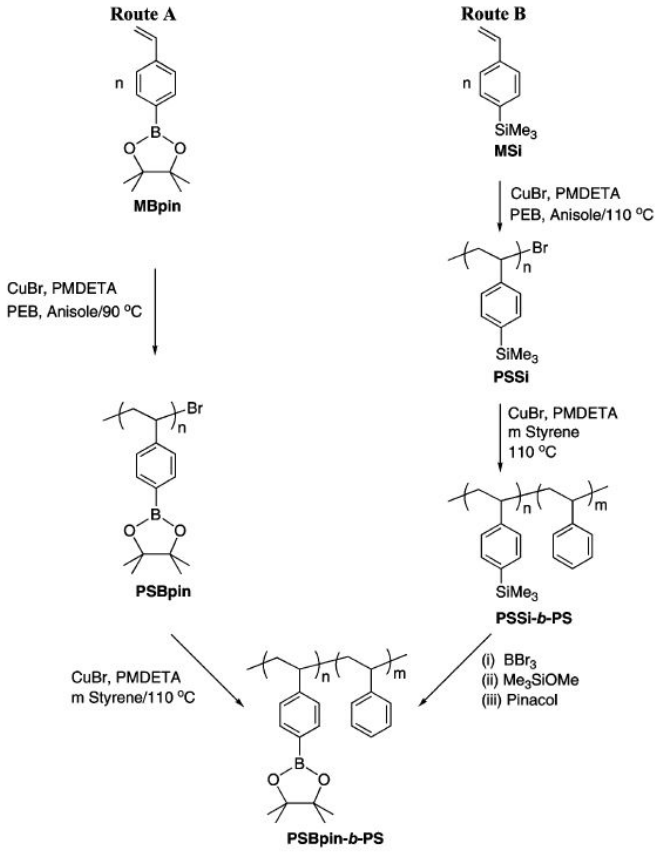

Scheme 1.1 Synthesis of the organoboron block copolymer PSBpin-*b*-PS by ATRP[21].

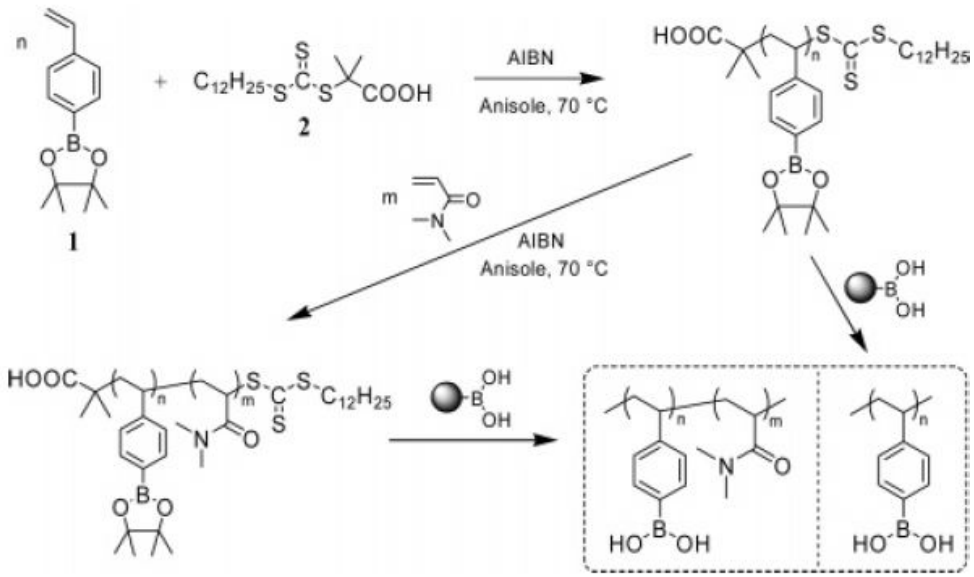

Scheme 1.2 Synthesis of boronic ester and boronic acid homopolymers and block copolymers by

RAFT polymerization[22].

1.4 Thesis Summary

In Chapter 2, since the first synthesis of styrene-boroxole monomer, there have been progresses in the synthesis, block copolymer characterizations such as binding constant and self-assembly behavior conditions, and potential application of self-regulating insulin delivery system. Chapter 3 describes the synthesis and characterization of new type of sugar-responsive polymers that are based on a sequence-specific copolymer and shows the feasibility of using these polymersomes as drug delivery vehicles

References

1. Meng, F.; Zhong, Z.; Feijen, *J. Biomacromolecules* **2009**, *10*, 197.
2. Li, M.-H.; Keller, P. *Soft Matter* **2009**, *5*, 927.
3. Wu, Q.; Wang, L.; Yu, H.; Wang, J.; Chen, Z. *Chem. Rev.* **2011**,*111*, 7855.
4. Jäkle, F. *Chem. Rev.* **2010**, *110*, 3985.
5. Kuivila, H. G. *J. Am. Chem. Soc.* **1954**, *76*, 870.
6. Lorand, J. P.; Edwards, J. O. *J. Org. Chem.* **1959**, *24*, 769.
7. Kataoka,K.; Miyazaki H.; Bunya M.; Okano T.; Sakurai Y. *J. Am. Chem. Soc.* **1998**, *120*, 12694
8. Roy, D.; Sumerlin, B. S. *ACS Macro Lett.* **2012**, *1*, 529.
9. Matsumoto, A.; Yamamoto, K.; Yoshida, R.; Kataoka, K.; Aoyagi, T.; Miyahara, Y. *Chem. Commun*. **2010**, *46*, 2203.
10. Matsumoto, A.; Ishii, T.; Nishida, J.; Matsumoto, H.; Kataoka, K.; Miyahara, Y. *Angew. Chem.,Int. Ed.* **2012**, *51*, 2124.
11. (a) Wulff, G. *Pure Appl. Chem*. **1982**, *54*, 2093–2102. (b) Burgemeister, T.; Grobe-Einsler, R.; Grotstollen, R.; Mannschreck, A.; Wulff, G. *Chem. Ber*. **1981**, *114*, 3403–3411. (c) Lauer, M.; Wulff, G. *J. Organomet. Chem*. **1983**, *256*, 1.

12. Kim, K. T.; Cornelissen, J. J. L. M.; Nolte, R. J. M.; van Hest, J. C. M. *J. Am. Chem. Soc.* **2009**, *131*, 13908.

13. Wang, J. S.; Matyjaszewski, K. *J. Am. Chem. Soc*. **1995**, *117*, 5614.

14. Kato, M.; Kamigaito, M.; Sawamoto, M.; Higashimura, T. *Macromolecules* 1995, 28, 1721.

15. Vogt, A. P.; Sumerlin, B. S. *Macromolecules* **2006**, *39*, 5286.

16. Chiefari, J.; Chong, Y. K.; Ercole, F.; Krstina, J.; Jeffery, J.; Le, T.P.T.; Mayadunne, R. T. A. ; Meijs, G. F.; Moad, C. L.; Moad, G.; Rizzardo, E.; Thang, S. H *Macromolecules* **1998**, *31*, 5559.

17. Perrier, S.; Pittaya, T. *J. Polym. Sci. Part A: Polym. Chem.* **2005**, *43*, 5347.

18. Moad, G.; Rizzardo, E.; Thang, S.H. *Aust J Chem* **2005**, *58*, 379.

19. Krasia, T.; Soula, R.; Borner, H.G.; Schlaad, H. Chem Commun **2003**, 538.

20. De P.; Gondi, S. R.; Sumerlin, B. S. *Biomacromolecules* **2008**, *9*, 1064.

21. Qin, Y.; Sukul, V.; Pagakos, D.; Cui, C.; Jäkle, F. *Macromolecules* **2005**, *38*, 8987.

22. Cambre, J.N.; Roy, D.; Gondi, S.R.; Sumerlin, B.S. *J. Am. Chem. Soc.* **2007**, *129*, 10348.

Chapter 2. Monosacchride-Responsive Disassembly of Polymersomes of Polyboroxole Block Copolymers at Neutral pH

2.1 Abstract

We synthesized the boroxole-containing styrenic monomer that can be polymerized by radical addition-fragmentation and chain transfer (RAFT) method. Polystyreneboroxole (PBOx) and its block copolymers with a poly(ethylene glycol) (PEG) as a hydrophilic block showed monosaccharide binding in phosphate buffer at neutral pH, which was quantified by Wang's competitive binding experiments. Amphiphilic block copolymers having a monosaccharide-responsive PBOx block self-assembled to polymersomes of which the average diameter was readily controllable by adjusting the number of boroxole units in the PBOx block via a controlled radical polymerization. These polymersomes also exhibited glucose-responsive disassembly at neutral pH. We demonstrated the possibility of using these polymersomes as glucose-responsive delivery vehicles for insulin at physiologically relevant pH medium.

2.2 Introduction

Polymersomes of amphiphilic block copolymers can store water-soluble cargos such as pharmaceutical molecules and polymers within the water-filled inner compartment.[1–3] Because the membrane of polymersomes consists of high molecular- weight polymers, polymersomes exhibit physical and chemical robustness at the expense of reduced transmembrane permeability.[4] Stimuli-responsive block copolymers readily change their physical properties in response to external stimuli such as temperature, pH, and irradiation.[5,6] The stimulated change of chemical and physical properties causes the vesicular membrane consisting of stimuli-responsive block copolymers to become permeable, resulting in release of the encapsulated cargo molecules from the polymersomes only when the appropriate stimulus is applied.[7] Therefore, polymersomes made from the self-assembly of stimuli-responsive block copolymers are promising candidates for smart nanocontainers that can be used as drug delivery vehicles and bioreactors.[8]

In this respect, of particular interest are polymers and block copolymers containing organoboronic acids, which bind reversibly to biologically important 1,2- and 1,3-diols such as monosaccharides and nucleotides.[9,10] This binding switches the solubility of boronic acid-containing polymers from insoluble to soluble in water, which can be translated into the monosaccharide- triggered swelling of hydrogels and disassembly of micelles and polymersomes.[11,12] Boronic acid-containing polymers, therefore, have been studied as candidate materials for sensors and drug delivery systems for sugar-

related human diseases such as diabetes.[13] Boronic acid−diol conjugates, however, easily hydrolyze in aqueous solutions at neutral pH, so boronic acid-containing polymers have been mainly used as sugar-responsive materials under high pH conditions (>9) that are incompatible with in vivo studies and applications. This drawback can be overcome when the pK_a of PBA is decreased using Wulff-type boronic acids[14,15] and phenylboronic acids with electron withdrawing moieties.[16] Hall and co-workers reported that the binding of phenylboroxole derivatives to glucose is superior to that of phenylboronic acids and Wulff-type boronic acids in aqueous solution at neutral pH.[17] The increased binding of boroxole to glucose in water arises from the fact that boroxole binds to pyranose-form saccharides such as glucopyranoside, a major form of glucose in neutral aqueous solution. Kiser and co-workers recently reported boroxole-functionalized polymers that mimic lectins to bind glucoproteins.[18] However, well-defined self-assembling block copolymers containing polyboroxole as a saccharide-responsive polymeric domain have not yet been synthesized.

We report here the first synthesis of the boroxole-containing styrenic monomer **1** and its controlled radical polymerization via the reversible addition−fragmentation and chain transfer (RAFT) method. Synthesized poly(styreneboroxole) (PBOx) showed binding to monosaccharides in phosphate buffer at neutral pH (pH 7.4), which was quantitatively studied using Wang's competitive binding assay.[19] By virtue of a controlled radical polymerization of **1**, we synthesized a series of sugar responsive block copolymers that self-assembled to form polymersomes in water. We demonstrated that the polymersomes of these block copolymers could encapsulate water soluble cargo molecules such as insulin, which could then be released from the polymersomes only in response to the presence of monosaccharides in aqueous solution under physiological pH conditions (Figure 2.1)

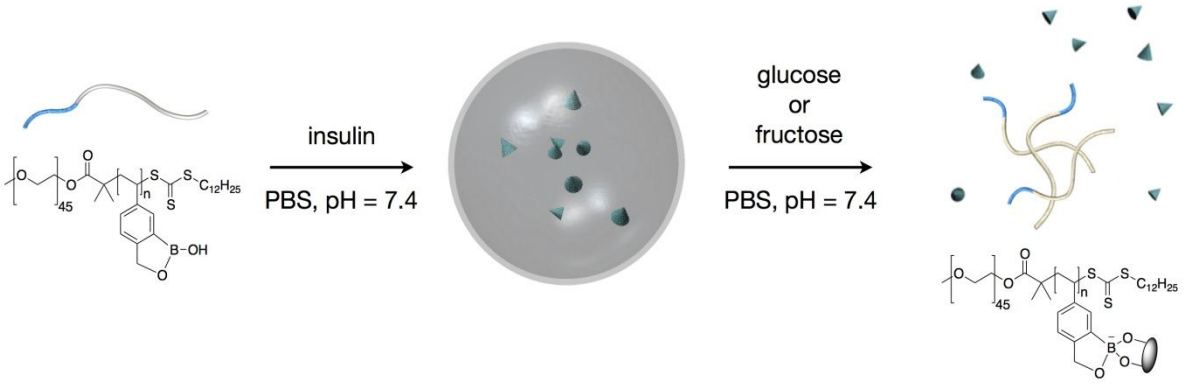

Figure 2.1 Self-assembly of **PEG-*b*-PBOx** and its disassembly in the presence of monosaccharides.

2.3 Results and Discussion

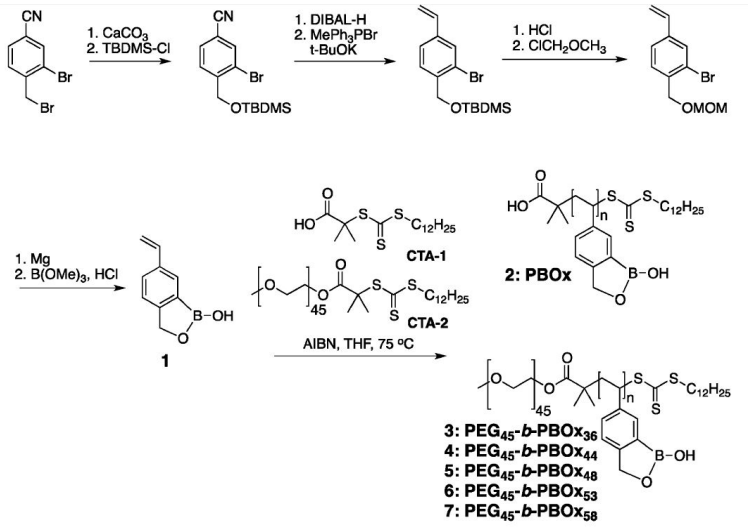

Scheme 2.1 Synthesis of monomer **1** and its homopolymer and block copolymers by RAFT polymerization.

Synthesis of the Boroxole-Containing Styrenic Monomer and Its Homopolymer and Block Copolymers. Styreneboroxole **1** was synthesized from 3-bromo-4- (bromomethyl)benzonitrile in seven steps in a moderate yield (Scheme 2.1).[15,20] During the synthesis, the protecting group for benzyl alcohol was switched from a tert-butyldimethylsilyl (TBDMS) group to a methoxymethyl (MOM) group because of the difficulty in deprotection after addition of boronic acid. Hydrolysis of methylborate in the presence of HCl removed a MOM group from the monomer in situ, yielding a crystalline solid of **1**

For the polymerization of **1**, we adopted a RAFT polymerization method using the trithiocarbonate chain transfer agent CTA-1 (Scheme 2.1).[21] Under the standard conditions ([CTA]:[1]:[AIBN] = 1:100:0.1) in tetrahydrofuran (THF) at 75 °C in a closed reaction vessel, RAFT polymerization of **1** showed a near-linear increase of conversion over time up to ~50% (Figure 2.2A). We also synthesized a series of amphiphilic block copolymers of PBOx by performing a RAFT polymerization of 1 with a poly(ethylene glycol) (PEG) based macro-chain-transfer agent (CTA-2, Scheme 2.1)[22] in THF ([CTA]:[1]:[AIBN] = 1:100:0.2) at 75 °C. The polymerization was quenched when the degree of polymerization (DP) of **1** reached the required value, as monitored by ^{1}H NMR integration of the reaction mixture. For all cases, the isolated yields of polymers and block copolymers after purification were 67−82% compared with the yield calculated by assuming the complete consumption of the chain-transfer agent.

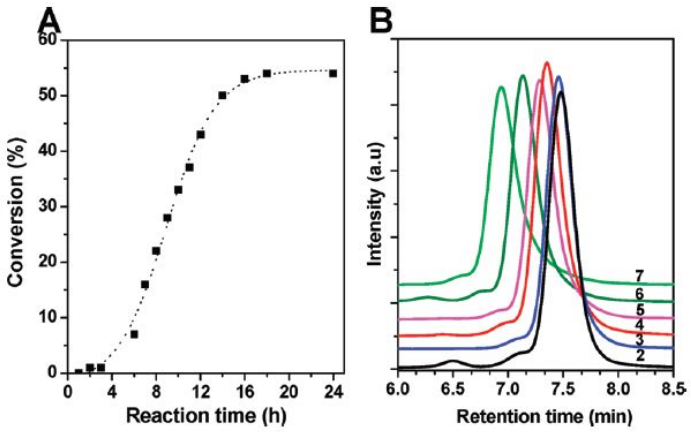

Figure 2.2 (A) Time−conversion plot for polymerization of **1** under RAFT conditions. (B) GPC traces of synthesized PBOx and PEG_{45}-*b*-$PBOx_n$ (**2**−**7**) (DMF, 65 °C).

Gel-permeation chromatography (GPC) of the block copolymers **3**−**7** [N,N-dimethylformamide (DMF), 65 °C] showed unimodal peaks with narrow polydispersity index (PDI) free from the peak of the PEG macro-chain-transfer agent, indicating successful chain extension from the PEG chain-transfer agent (Figure 2.2B). The molecular weight and DP of the PBOx block were estimated by ^{1}H NMR integration using the methylene peak of PEG as a standard (Table 1 and Figure 2.3). The molecular weights obtained by GPC using polystyrene standards were consistently larger than those measured by ^{1}H NMR analysis. Attempts to obtain MALDI−TOF mass spectra were unsuccessful.

Table 2.1. Characterization of homopolymer (PBOx) **2** and PEG_{45}-*b*-$PBOx_n$ Block Copolymers **3-7**

sample	M_n (g/mol)[a]	DP_n (PBOx)[b]	M_n (g/mol)[c]	PDI[c]	K_a^{fru} (M^{-1})[d]	K_a^{glu} (M^{-1})[d]
2	-	-	**21,400**	**1.06**	**643.3**	**14.5**
3	**8420**	**38**	**23,100**	**1.04**	-	-
4	**9400**	**44**	**26,100**	**1.06**	-	-
5	**10020**	**48**	**28,300**	**1.06**	-	-
6	**10840**	**53**	**34,900**	**1.06**	-	-
7	**11640**	**58**	**43,200**	**1.10**	**420.1**	**9.9**

[a] The number average molecular weight determined by ^{1}H NMR integration. [b] The number average degree of polymerization of PBOx determined by ^{1}H NMR integration. [c] The number average molecular weight and polydispersity index obtained by GPC (DMF, 65 °C, 1 mL/min flow rate) using PS standards. [d] Association constants measured by the Wang's method.

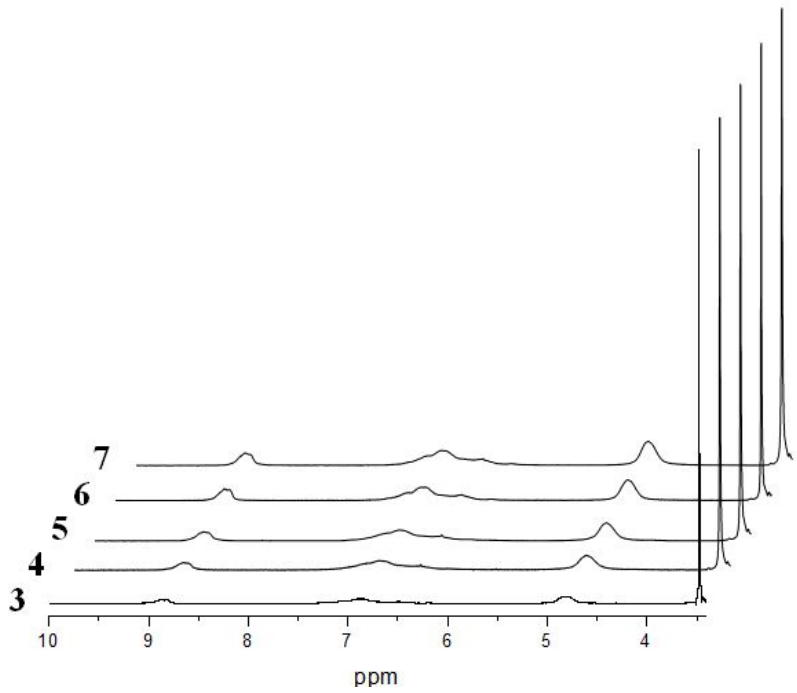

Figure 2.3 ^{1}H NMR (600 MHz, DMSO-d_6) spectra of block copolymers PEG_{45}-*b*-$PBOx_n$ (**3**: n = 38, **4**: n = 44, **5**: n = 48, **6**: n = 53, **7**: n = 58). The degree of polymerization of the PBOx block was calculated by comparing the integration of the benzyl signal of the PBOx (4.8 ppm) and the methylene signal of the PEG (3.5 ppm).

Binding Constant of Homopolymer and Block Copolymers with Monosaccharides. To chracterize this binding, we performed Wang's competitive binding assay to quantitate the binding of PBOx to monosaccharides.[19] The absorption at 452 nm of the initial PBOx/Alizarin red S (ARS) complex ([boroxole]:[ARS] = 250:1) in a 9:1 (v/v) phosphate buffer/dioxane mixture (pH 7.4) shifted to 520 nm upon addition of fructose (0.5 M) and glucose (0.5 M), indicating the replacement of boroxole-bound ARS molecules with monosaccharides (Figures 2.4). The association constant K_a of PBOx was assessed by measuring the decrease in fluorescence emission of the PBOx/ARS complex caused by the replacement of ARS molecules bound to PBOx by monosaccharides. The measured K_a for homopolymer **2** was 643.3 M^{-1} for fructose and 14.5 M^{-1} for glucose; for the representative block copolymer 7, K_a = 420.1 M^{-1} for fructose and 9.9 M^{-1} for glucose. These K_a values are comparable to the results reported for benzoboroxole- and boroxole-functionalized polymers[17,18] indicating that boroxoles incoporated into the polymeric backbone exhibit binding to monosaccharides comparable tomthat of phenylboroxole.

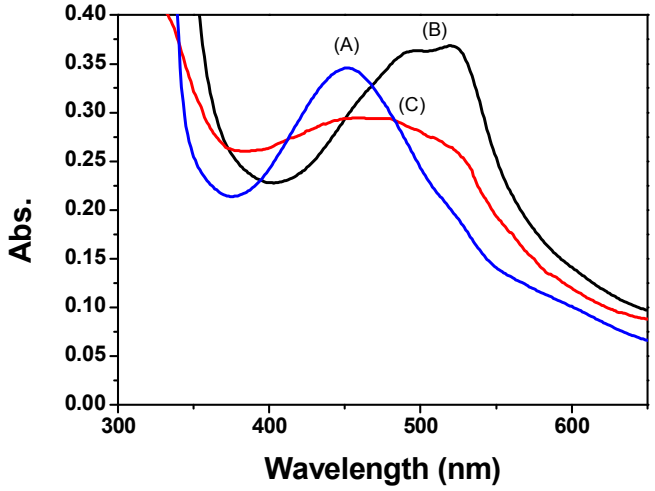

Figure 2.4 (A) Absorbance of a ARS (8×10^{-5} M in pH 7.4, 0.1 M phosphate buffer) with PBOx (0.02 M) (B) ABS (8×10^{-5} M) with 0.02 M PBOx and 0.5 M fructose (C) 8×10^{-5} M ARS with 0.02 M PBOx and 0.5 M glucose.

Self-Assembly of Block Copolymers. The monosaccharide-responsive behavior of PBOx at neutral pH makes this polymer an ideal candidate for constructing stimuli-responsive block copolymers that self-assemble into polymersomes capable of encapsulating pharmaceutical cargos such as insulin. To the best of our knowledge, there have been no reports describing boronic acid-containing block copolymers that form polymer vesicles and exhibit sugar-responsive release of cargo in water at physiologically relevant pH. To guide the self-assembly of block copolymers into polymersome formation, the ratio between the hydrophilic and hydrophobic blocks had to be optimized. Therefore, we studied the self-assembly behavior of our block copolymers in water. Self-assembled structures of block copolymers **3**–**7** were prepared by the selective solvent method: to a THF solution (2 mL) of PEG-*b*-PBOx (0.5 wt %) was slowly added distilled water at a rate of 2 mL/h with stirring until the water content reached 66%. The resulting suspension was dialyzed against water for 24 h and then characterized by transmission electron microscopy (TEM) and dynamic light scattering (DLS).

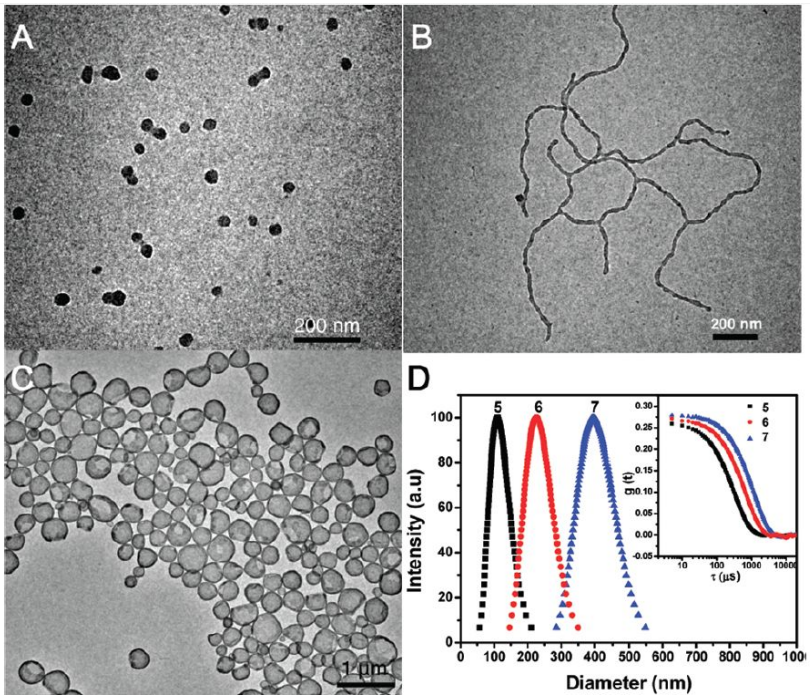

Figure 2.5 (A−C) TEM images of micelles and polymersomes formed by self-assembly of PEG-b-PBOx in water. (A) Spherical micelles of **3**. (B) Cylindrical micelles of **4** [average diameter (D_{av}) = 42 nm, PDI = 1.20]. (C) Polymersomes of 7. (D) Size distributions and (inset) autocorrelation functions of polymersomes of **5**−**7** in water. D_{av} (PDI) for polymersomes: **5**, 114 nm (0.103); **6**, 232 nm (0.102); **7**, 387 nm (0.064).

A series of block copolymers **3**−**7** showed self-assembly behavior similar to that of conventional amphiphilic block copolymers: as the DP of the sugar-responsive PBOx block increased, the morphology of the self-assembled structures changed from spherical micelles (**3**, Figure 2.5A) to cylindrical micelles (**4**, Figure 2.5B) to polymersomes (Figure 2.5C). Interestingly, block copolymers **5**−**7** formed polymersomes whose diameters, as measured by DLS, were strongly dependent on the number of boroxole repeating units in the PBOx block. As shown in Figure 2.5D, the average diameter determined by DLS ranged from 114 to 387 nm with increasing DP of the PBOx block (for TEM images, Figure 2.6). All of the micelles and polymersomes were stable in water for more than 3 months, as evidenced by TEM and DLS experiments showing no change in morphology or diameter.

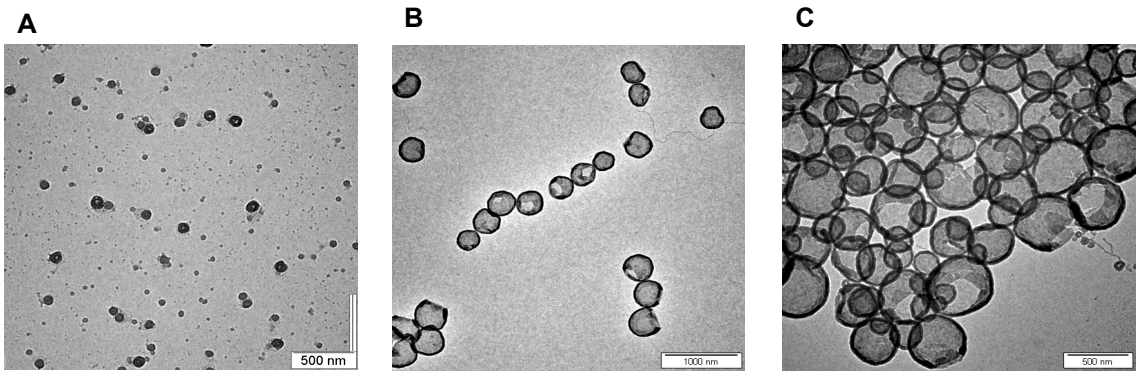

Figure 2.6 TEM images of polymersomes of (A) **5** (PEG_{45}-*b*-$PBOx_{48}$), (B) **6** (PEG_{45}-*b*-$PBOx_{53}$), and (C) **7** (PEG_{45}-*b*-$PBOx_{58}$).

Glucose-Responsive Behavior of the Polymersomes. The sugar-responsive disassembly of polymersomes of PEG-*b*-PBOx was examined by measuring the turbidity of polymersome solutions in the presence of monosaccharides at neutral pH (Figure 2.7). The optical transmittance at 580 nm of the turbid suspension of polymersomes of **7** was monitored in the presence of monosaccharides. With 0.2 M fructose, the turbidity of the polymersome solution (pH 7.4) decreased as a result of disassembly of the polymersomes into block copolymers caused by binding of monosaccharides to PBOx. This sugar-responsive bahavior of polymersomes of **7** in the presence of monosaccharides was also observed from the disappearance of polymersomes after addition of monosaccharides (0.2 M fructose) in the DLS study (Figure 2.8). The disassembly of polymersomes in the presence of glucose was expected to be slower and required a higher concentration of sugar, as suggested by the Wang's assay with **7** (Table 2.1). Upon dialysis against pure water, a polymersome solution of **7** formed precipitates due to the dissociation of boronate esters of saccharide molecules and boroxoles, indicating the reversible interaction between boroxoles and saccharides.

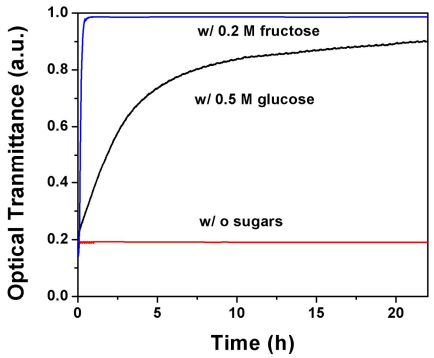

Figure 2.7 Optical transmittance profiles of the polymersome solution of **7** in the presence of monosaccharides.

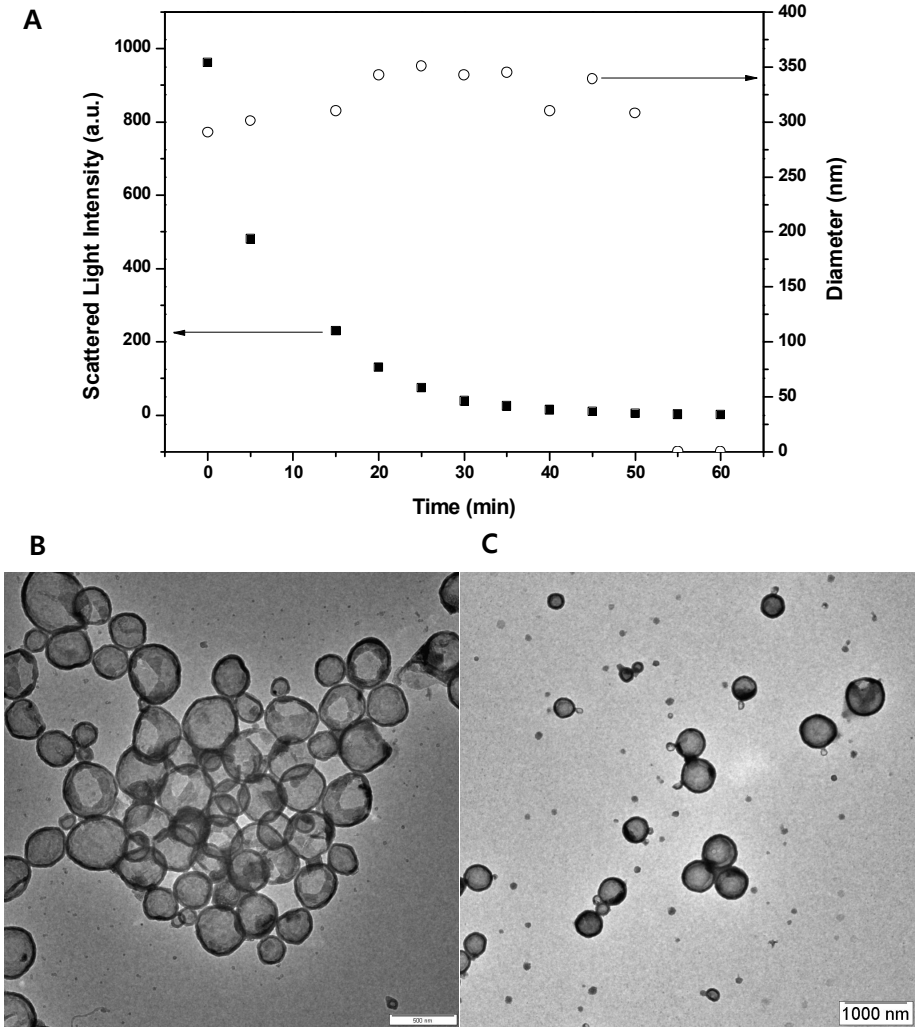

Figure 2.8 (A) Scattered light intensity and diameter change of polymersome solution of 7 in the presence of fructose (0.2 M) in phosphate buffer (pH = 7.2). (B) A representative TEM image of polymersomes of 7 without fructose. (C) A representative TEM image of the same polymersomes in the presence of fructose (The sample was taken 15 min after introduction of fructose to the polymersome solution. Before TEM sampling, the solution was diluted with water and dialyzed against water for 24 h.).

Fluorescein-Labeled Insulin Encapsulation in the Polymersome. To demonstrate the possibility of using these saccharideresponsive polymersomes as sugar-responsive smart nanocontainers for water-soluble molecules, we encapsulated fluorescein isothiocyanate (FITC)-labeled human insulin (F-insulin) within polymersomes. For encapsulation, an aqueous solution of F-insulin (0.1 mg/mL in

phosphate buffer) was slowly added to the THF solution of **7** to induce self-assembly of block copolymers into polymersomes in the presence of F-insulin. The resulting polymersome solution was purified by dialysis (MW cutoff of 13 000 Da) against phosphate buffer for 2 days. To remove any unencapsulated F-insulin, polymersome solutions (D_{av} = 340 nm, PDI = 0.204) were further purified using size-exclusion chromatography (Sephadex G-50). Encapsulation of F-insulin within polymersomes was confirmed by laser confocal fluorescence microscopy (LCFM), which showed green fluorescence emanating from the polymersomes (Figure 2.9). After purification, polymersomes encapsulating F-insulin were stable in acidic solution (1 < pH < 7) for at least 24 h without any disassembly or aggregation of polymersomes, as monitored by DLS.

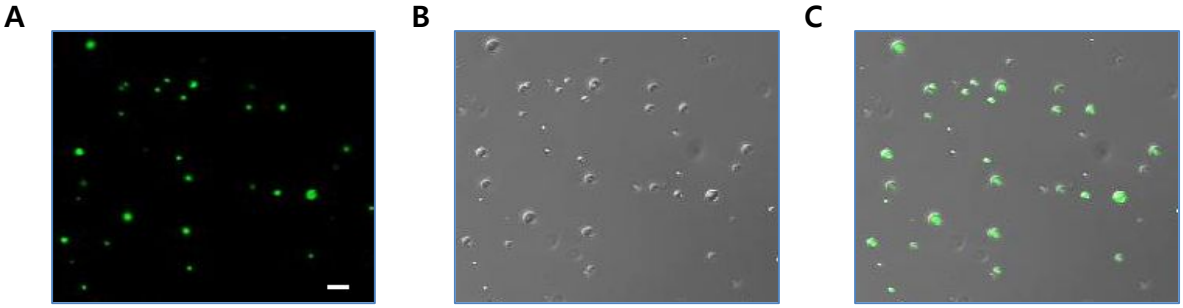

Figure 2.9 LCFM images of polymersomes of **7** encapsulating FITC-labeled human insulin : (A) dark-field (B) bright-field (C) merged. Scale Bar: 5 μm.

Feasibility of the Polymersomes as Insulin Delivery Vehicles in Physiologically Relevant Conditions. As summarized in Figure 2.1, encapsulated F-insulin was released from polymersomes in response to the presence of monosaccharide in the medium (pH 7.4). The solution of polymersomes of **7** (1 mL) encapsulating F-insulin was charged in a dialysis bag (MW cutoff of 10 000 Da), which was then dialyzed against 100 mL of phosphate buffer containing fructose (0.1 M) or glucose (0.3 M). During dialysis, a fraction of the buffer solution was taken at intervals of 30 min for fluorescence measurements. The release of F-insulin from disassembled polymersomes was observed from the measurement of emission spectra (λ_{max} = 518 nm), which showed an increase over the period of dialysis (Figure 2.10). Without monosaccharides, no fluorescence was observed during dialysis of polymersomes encapsulating F-insulin over the entire time period of dialysis, indicating that polymersomes of PEG-*b*-PBOx did not release the encapsulated insulin without triggering by monosaccharide binding. Also, the presence of nonbinding diols such as ethylene glycol in the medium (up to 1 M) did not cause significant disassembly of the polymersomes. The polymersomes, as examined by DLS, stayed intact during 2 days of dialysis in the presence of 1 M ethylene glycol.

As suggested by previous studies,[17,18] nonreducing sugars such as α-methyl-D-mannopyranoside also induced disassembly of the polymersomes, as indicated by the release of F-insulin. In the presence of monosaccharides, 50% of the release of insulin from the polymersomes of **7** was achieved within 1.4 h with 0.1 M fructose and 10.5 h with 0.3 M glucose.

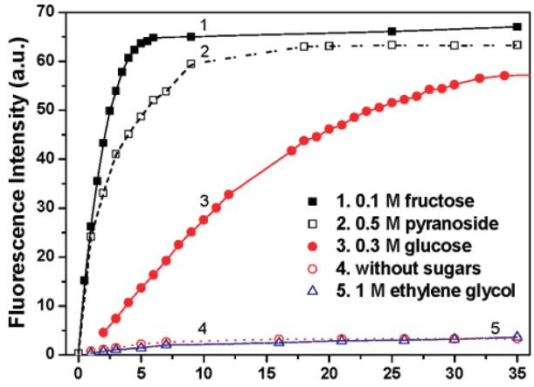

Figure 2.10 Release profiles of F-insulin from the polymersomes of **7** in the presence of monosaccharides and nonbinding diols.

2.4 Summary

In summary, we have synthesized a boroxole-based styrenic monomer that can be polymerized by the RAFT method. The controlled polymerization of the boroxole-based monomer **1** with a PEG-based chain-transfer agent allowed us to synthesize well-defined monosaccharide-responsive block copolymers. By utilizing the sugar-responsive disassembly of polymersomes of PEG-*b*-PBOx in aqueous solution at neutral pH, we have demonstrated the monosaccharide-triggered disassembly of polymersomes to release encapsulated cargo molecules such as FITC-labeled insulin under physiologically relevant pH conditions. Encapsulated insulin was released from the polymersomes only in response to the presence of monosaccharides that bind to boroxole moieties. The boroxole containing polymers and block copolymers reported here may find applications in the development of sensors and drug delivery systems designed for glucose-related human diseases such as diabetes.

2.5 Experimental

General Method. All reagents and chemicals were purchased from commercial sources and used as received. All reactions were performed under N_2 unless otherwise noted. NMR spectra were recorded on a Varian VNMRS 600 spectrometer with $CDCl_3$ and DMSO-d_6 as a solvent. Molecular weights of block copolymers were measured on a Agilent 1260 Infinity GPC system equipped with a PL gel 5 μm mixed B column (Polymer Laboratories)) and differential refractive index detectors. DMF was used as an eluent with a flow rate of 1 mL/min. A PS standard (Polymer Laboratories) was used for calibration. A Cary Eclipse Fluorescence Spectrophotometer was used for all fluorescence studies. The ARS fluorescence intensities were measured with an excitation wavelength of 468nm and an emission wavelength of 572nm. The insulin fluorescent intensities were measured with excitation wavelength of 495 and emission wavelength of 518 nm. Transmission electron microscopy (TEM) was performed on a JEOL 1400 microscope at an acceleration voltage of 120 kV. Sample specimens were prepared by placing a drop of the solution on a carbon-coated Cu grid (200 mesh, EM science). After 30 min, the remaining solution on a grid was removed with a filter paper, and the grid was air-dried for 8 h. Dynamic light scattering (DLS) experiments were carried out on a BI-200SM equipped with a diode laser (637 nm, 4 mW). All DLS data were handled on a Dispersion Technology Software (Brookhaven Instruments). Optical transmittance of the solutions was measured on a on a JASCO V-670 UV-Vis spectrophotometer equipped with a thermostat sample holder with a magnetic stirrer. % Transmittance at 580 nm was used to calculate the optical transmittance (O.T) of the solution by the following equation. $O.T = 1 - ((T_{buf} - T_{sol})/T_{buf})$ where T_{buf} was the % transmission of the buffer at 580 nm and T_{sol} was the % transmittance of the solution at the same wavelength. Confocal Laser Scanning Fluorescence Microscopy (CLSM) was performed on a FluoView 1000 Confocal Microscope (Olympus).

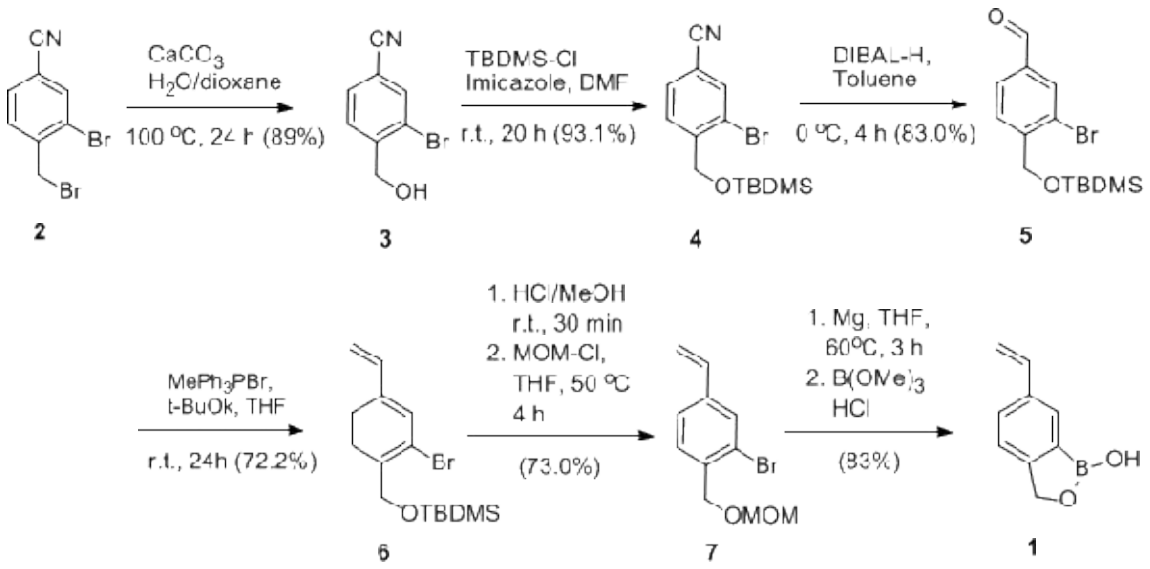

Synthesis of Styreneboroxole 1.

3-bromo-4-hydroxymethylbenzonitrile (3). 3-bromo-4-bromomethylbenzonitrile (**2**) (11.6 g, 42.5 mol) was added to a suspension of $CaCO_3$ (18.3 g) in dioxane/water (2:3 v/v, 350 mL). This mixture was stirred at 100 °C for 24 h. After cooling to room temperature, the reaction mixture was extracted with diethyl ether (100 mL, 3 times). The combined organic phase was washed with brine and water. The organic layer was dried over anhydrous sodium sulfate. After solvent removal with a rotavap, the resulting solid was recrystallized in CH_2Cl_2/MeOH (95:5 v/v). Colorless crystalline solid was obtained. Yield 8.1 g (89 %). ^{1}H NMR (600 MHz, $CDCl_3$) δ 7.81 (s, 1H), 7.69 (d, J = 7.8 Hz, 1H), 7.64 (d, J = 7.8 Hz, 1H), 4.79 (s, 2H); ^{13}C NMR (150 MHz, $CDCl_3$) δ = 145.4, 135.4, 131.2, 128.4, 121.9, 117.3, 112.5, 64.2; MS (EI) calcd. for $C_8H_6O_1Br_1N_1$ 212.04; found 212.03.

3-Bromo-4-((tert-butyldimethylsilyloxy)methyl)benzonitrile (4). A TBDMS-Cl (6.9 g, 46 mmol) in dry DMF solution (80 mL) was added dropwise to a 3-bromo-4-hydroxymethylbenzonitrile (**3**) (8.1 g, 38.3mmol) and imidazole (6.5 g, 95.8 mmol) in dry DMF solution. The reaction mixture was stirred at room temperature for 20 h. The reaction was quenched by adding water (50 mL) and the reaction mixture was extracted with diethyl ether (100 mL) three times. The combined organic layer was washed with brine and water. After drying the solution with anhydrous $MgSO_4$, the filtered solution was concentrated by removing the solvent with a rotavap. A white solid was obtained. The purity was checked by ^{1}H NMR and the resulting compound was used without further purification. Yield 11.68 g (93.1%). ^{1}H NMR (600 MHz, $CDCl_3$) δ 7.78 (d, J=1.6 Hz, 1H), 7.69 (d, J = 7.8 Hz, 1H), 7.64 (dd, J = 1.6Hz and 7.8 Hz, 1H), 4.73 (s, 2H), 0.96 (s, 9H), 0.15 (s, 6H); ^{13}C NMR (150 MHz, $CDCl_3$) δ = 151.6, 140.4, 136.4, 133.3, 126.3, 122.9, 117.3, 69.7, 31.2, 23.7, -5.3; MS (ESI) calcd. for $C_{14}H_{20}O_1Br_1N_1Si_1$ $[M+Na]^+$ 349.30; found 349.78.

3-Bromo-4-((tert-butyldimethylsilyloxy)methyl)benzolaldehyde (5). Compound **4** (11.68g, 35.8 mmol) was dissolved in 100ml dry toluene. Then, the solution was cooled to 0 °C in an ice/water bath.

To this cooled solution was added a toluene solution of DIBAL-H (1 M, 60 mL) via a cannula with stirring. The reaction mixture was stirred at 0 °C for 3 h. The reaction was quenched by adding methanol dropwise (60mL), dilute HCl (1 M), and THF. The organic layer was collected, washed with brine, and dried with anhydrous $MgSO_4$. After filtration, the filtered solution was concentrated on a rotavap. The crude mixture was purified by silica gel column chromatography (hexane:ethyl acetate 15:1 v/v). Colorless oil was obtained. Yield 10.1 g (83.0 %). ^{1}H NMR (600 MHz, $CDCl_3$) δ 9.79 (s, 1H), 7.84 (s, 1H), 7.69 (d, J = 7.8 Hz, 1H), 7.60 (d, J = 7.8 Hz, 1H), 4.61 (s, 2H), 0.82 (s, 9H), 0.16 (s, 6H); ^{13}C NMR (150 MHz, $CDCl_3$) δ = 191.5, 147.2, 136.4, 132.7, 128.7, 127.8, 121.4, 64.6, 25.9, 19.3, -5.4; MS (ESI) calcd. for $C_{14}H_{21}O_2Br_1Si_1$ $[M+H]^+$ 329.30; found 329.81.

3-Bromo-4-((tert-butyldimethylsilyloxy)methylstyrene (6). Methyltriphenylphosphonium bromide (14.2 g, 39.8 mmol) was dissolved in dry THF (300 mL). The flask was vacuumed and refilled with N_2 three times. A dry THF solution of potassium t-butoxide (5.2 g, 45 mmol) added to the flaks via a syringe. A color change from white to reddish orange was observed and the mixture was stirred for 1 h. A THF solution of **5** (10.1 g, 31 mmol) was then added to the mixture. The mixture was stirred at R.T for 24 h. The solvent was removed under reduced pressure and the resulting crude mixture was dissolved in CH_2Cl_2. This solution was washed with water and brine. The organic layer was collected and dried with anhydrous $MgSO_4$. After removing the solvent on a rotavap, the crude mixture was purified by silica gel column chromatography (hexane:ethyl acetate = 20:1). Colorless oil was obtained. Yield 7.8 g (72.2 %). ^{1}H NMR (600 MHz, $CDCl_3$) δ 7.55 (s, 1H), 7.51 (d, J = 7.8 Hz, 1H), 7.36 (d, J = 7.8 Hz, 1H), 6.65 (dd, J_1 = 10.8 Hz, J_2 = 18.1 Hz, 1H), 5.74 (d, J = 18.1 Hz, 1H), 5.27 (d, J = 10.8 Hz, 1H), 4.74 (s, 2H), 0.98 (s, 9H), 0.14 (s, 6H); ^{13}C NMR (150 MHz, $CDCl_3$) δ = 134.2, 132.5, 129.9, 124.2, 122.1, 119.7, 115.7, 109.2, 59.1, 20.4, 12.9, -5.4; MS (ESI) calcd. for $C_{15}H_{23}O_1Br_1Si_1$ $[M+Na]^+$ 350.33; found 350.77.

3-Bromo-4-((methoxymethoxy)methyl)styrene (7). Compound **6** (7.8 g, 24 mmol) was dissolved in methanol (150 mL). A few drops of conc. HCl was added to this solution, and the solution was stirred at room temperature for 30 min. The reaction mixture was extracted with diethyl ether 3 times. The combined organic phase was washed with brined and water, and dried with anhydrous $MgSO_4$. After filtration and evaporation of the solvent, white crystalline solid was obtained. Purity of this compound was checked with ^{1}H NMR. This solid, 3-bromo-4-hydroxymethylstyrene was used for the next reaction without further purification. 3-bromo-4-hydroxymethylstyrene (5.0 g, 23.4 mmol) was dissolved in dry THF (20 mL) and the solution was cooled to 0 °C. To this cooled solution was added at once sodium hydride (60 wt % dispersed in mineral oil, 1.09 g, 25.7 mmol). The reaction mixture was stirred at 0 °C for 20 min. A THF solution of methoxymethyl chloride (2.13 mL, 28 mmol in 15 mL THF) was added dropwise via a syringe. The reaction mixture was warmed to room temperature and stirred for 2 h at room temperature. Then, the reaction was further proceed at 70 °C for 3 h. The

reaction was quenched by adding 10 % (w/w) aqueous solution of Na_2CO_3. The quenched reaction mixture was concentrated on a ratavap and the crude mixture was diluted with CH_2Cl_2. This solution was extracted with water three times. After drying the organic phase with anhydrous $MgSO_4$, the solvent was removed on a rotavap. The crude compound was further purified by silica gel column chromatography (hexane:ethyl acetate = 15:1). The product was obtained as colorless oil. Yield 4.4 g (73.0%). ^{1}H NMR (600 MHz, $CDCl_3$) δ 7.60 (d, *J*=1.6 Hz, 1H), 7.44 (d, *J* = 7.8 Hz, 1H), 7.34 (dd, *J* = 1.6 Hz and 7.8 Hz, 1H), 6.64 (dd, J_1 = 10.8 Hz, J_2 = 18.1 Hz, 1H), 5.76 (d, *J* = 18.1 Hz, 1H), 5.29 (d, *J* = 10.8 Hz, 1H), 4.76 (s, 2H), 4.66 (s, 2H), 3.43 (s, 3H); ^{13}C NMR (150 MHz, $CDCl_3$) δ = 143.4, 135.4, 131.0, 128.8, 122.2, 117.3, 112.5, 96.4, 68.2, 55.6; MS (ESI) calcd. for $C_{15}H_{23}O_1Br_1Si_1$ $[M+Na]^+$ 350.33, found 349.77.

4-vinylboroxole (1). Mg (1.0 g, 41.7 mmol) was placed in a two neck flask equipped with a reflux condenser. The flask was vacuumed and refilled N_2 three times. Under N_2 atmosphere, dry THF (70 mL) was added to this flask. A bulk 7 (4.4 g, 17 mmol) was added to the flask slowly via a syringe. The reaction was initiated and preceded for 1 h. Then, the reaction was further stirred at 60 °C for 3 h. The reaction mixture was then cooled to -76 °C in a dry ice/acetone bath. To this cooled solution was added trimethyl borate (3.8ml, 34mmol) dropwise via a syringe. After addition, the reaction mixture was warmed up slowly to room temperature and stirred for 8 h at room temperature. The reaction was quenched by adding aqueous HCl (2 M, 35 mL). The organic layer was separated from the aqueous layer, which was extracted with $CHCl_3$ (100 mL, 3 times). The $CHCl_3$ layer was collected and combined. The combined organic solution was evaporated on a rotavap. The crude mixture was purified by silica gel column chromatography (hexane:ethyl acetate = 3:1 v/v). A white crystalline solid was obtained. Yield 2.26 g (83.0%). ^{1}H NMR (600 MHz, DMSO-D_6) δ 9.17 (s, 1H), 7.78 (d, *J*=1.6 Hz 1H), 7.60 (dd, *J* = 1.6 Hz and 7.8 Hz, 1H), 7.39 (d, *J* = 7.8 Hz, 1H), 6.82 (dd, J_1 = 10.8 Hz, J_2 = 18.1 Hz, 1H), 5.83 (d, *J* = 18.1 Hz, 1H), 5.27 (d, *J* = 10.8 Hz, 1H), 4.98 (s, 2H). ^{13}C NMR (150 MHz, DMSO-d6) δ = 154.0, 137.2, 136.2, 128.9, 128.5, 122.0, 114.2, 70.3. HRMS calcd. for $C_9H_9O_2B_1$ 160.0697, found 160.0695.

RAFT Polymerization of 6-vinylboroxole.

CTA-1 was synthesized according to the literature procedure.[23]

CTA-2. methoxy poly(ethylene glycol) (Mn = 2000 g/mol, Aldrich) was used to synthesize a macro-chain transfer agent.[24]

^{1}H NMR (600 MHz, $CDCl_3$) δ 4.25 (t, 2H), 3.64(m, 178H), 3.38 (s, 3H), 3.26 (t, 2H), 1.70 (s, 6H), 1.23-1.40 (m, 20H), 0.88 (t, 3H).

Polystyrene boroxole (PBOx). 6-vinylboroxole (**1**) (200 mg, 1.25 mmol) and **CTA-1** were charged in a Schlenk tube with a magnetic stir bar. This tube was vacuumed and charged with N_2 three times. To this mixture was added 5 mL of dry THF. The solution was degassed by bubbling N_2 for 15 min. A

THF solution of AIBN (0.2 mg, mmol in 0.2 mL) was added at once to this solution, which, then, was immersed into a preheated oil bath (75 °C). The Schlenk tube was sealed, and the polymerization was performed for 17 h at 75 °C. For kinetic studies, a fraction of the reaction mixture was taken via a syringe under N_2. The conversion of **1** to **PBOx** was measured by taking integration of ^{1}H NMR signal. After polymerization, the reaction mixture was exposed to air and immersed in the ice-water bath. The solution was precipitated into cold diethyl ether. The precipitates were collected by filtration, which were washed profusely with CH_2Cl_2 and vacuum dried.

Synthesis of Block Copolymers PEG-b-PBOx. The same procedure for PBOx polymerization was used for the synthesis of block copolymers using **CTA-2** as a chain transfer agent.

Table 2.2 Isolated yield of polymers and homopolymers after purification.[a]

sample	[1]:[CTA]:[I]	Conversion (%)	DP_n (^{1}H NMR)	Yield (mg)[a]	CTA efficiency (%)[b]
2	100:1:0.1	43	-	40	-
3	100:1:0.2	43	38	34	79
4	100:1:0.2	47	44	32	68
5	100:1:0.2	53	48	38	71
6	100:1:0.2	52	53	35	67
7	100:1:0.2	50	58	41	82

[a] all polymerization was performed with 100 mg of monomer **1**. [b] CTA efficiency was calculated with the isolated yield and the theoretical yield calculated by assuming all CTA being used for polymerization.

Preparation of Micelle and Polymersome Solutions. Doubly distilled water (MilliQ, 18.1 MΩ) was used throughout the experiments. A typical procedure is described: PEG_{44}-b-$PBOx_{58}$ (10 mg) was dissolved in THF (2 mL) in a 15 mL capped vial with a magnetic stirrer. The solution was stirred for 3 h at room temperature. A syringe pump was calibrated to deliver water at a speed of 2 mL/h. The vial cap was replaced by a rubber septum. 4 mL of water was added to the organic solution with vigorous stirring (850 rpm) by a syringe pump with a 5 mL syringe equipped with a steel needle. The remaining

solution was subjected to dialysis (SpectraPor, molecular weight cut-off: 12,000−14,000 Da) against water for 24 h with a frequent change of water. The resulting suspension was collected from a dialysis bag. The diameter and morphology of polymersomes were studied by dynamic light scattering (DLS) and TEM. If necessary, the medium was exchanged from water to phosphate buffer (0.1 M, pH = 7.4) by using a centrifugal filter (Amicon, 100 KDa membrane cut-off) to remove water. The concentrated polymersome solution was re-suspended in phosphate buffer.

Turbidity Test of Polymersomes. 5 mL of the polymersome solution (phosphate buffer, pH = 7.4) was charged in a quartx cuvette with a magnetic stir bar. To this solution was added fructose (180.16 mg, 1 mmol) or glucose (270.3 mg, 1.5 mmol) at once. After complete dissolution of added sugar, the pH of the solution was readjusted to 7.4 by adding aqueous NaOH (1M). 2 mL of this solution was charged in a quartz cuvette with a magnetic stirrer. The absorbance at 580 nm was measured in every 30 sec with a constant stirring. For measuring the scattered light intensity of the polymersome solution, the polymersome solution was stirred in the presence of 0.2 M fructose. A small portion (0.05 mL) of the polymersome solution was taken in every 5 min. This sample was instantly mixed with 1 mL of water. This diluted solution was used for the dynamic light scattering experiment. The scattered light intensity was measured at a fixed slit width throughout the measurement.

Fluorescein Labeling of Insulin. The stock solution of insulin was obtained by dissolving 1 mg of insulin (Human insulin, Sigma) in 0.1 mL of 1 % acetic buffer and the working solution of insulin (0.1 mg/mL) was obtained by diluting the stock solution by 100 folds into reaction buffer containing 50 mM NaH_2PO_4, 100 mM NaCl (pH 7.5). The working solution of insulin was incubated with 10 molar equivalents of *N*-hydroxysuccinimidyl ester (NHS) fluorescein at room temperature with vigorous shaking for one and half hours. Reactions were implemented to dialysis with sterile deionized water to remove unreacted NHS-fluorescein overnight.

Fluorescein-Labeled Insulin Encapsulation in the Polymersome. A PEG_{44}-b-$PBOx_{58}$ (8 mg) was dissolved in THF (2 mL) in a 15 mL capped vial with a magnetic stirrer. The solution was stirred for 3 h at room temperature. A syringe pump was calibrated to deliver Fluorescein-labeled Insulin (F-Ins) in phosphate buffer (0.3 mg/mL) a speed of 2 mL/h. The vial cap was replaced by a rubber septum. 4 mL of F-Ins Insulin was added to the organic solution with vigorous stirring (850 rpm) by a syringe pump with a 5 mL syringe equipped with a steel needle. The remaining solution was subjected to dialysis (SpectraPor, molecular weight cut-off: 12,000−14,000 Da) against phosphate buffer for 2days with a frequent change of phosphate buffer. The resulting suspension was collected from a dialysis bag, and the suspension was then purified by size exclusion column chromatography (Sephadex G-50), which showed two green bands. The first band was collected and combined.

Preparation and Analysis of Laser Confocal Fluorescence Microscopy Samples. The solution of polymersomes encapsulating fluorescein-labeled insulin was transferred onto chamlide (magnetic

chamber for 25 mm coverslip) and the images were taken directly. Confocal fluorescence images were acquired with FV1000 laser confocal fluorescence microscopy (Olympus) with the parameters of 10 % laser power (370 HV), 1 Gain and 21 % offset and excitation and emission wavelength of 494 and 518 nm, respectively. The images were viewed and processed with FV1000 viewer software (Olympus).

Release of Fluorescein-Insulin from Polymersomes of PEG-b-PBOx. All experiments were performed by the method described: A solution of polymersomes of **7** (PEG_{45}-*b*-$PBOx_{58}$) (1 mL) encapsulating fluorescein-labeled insulin was subjected to a dialysis bag (SpectraPor, molecular weight cut-off: 8,000 Da), which was dialyzed against 100 mL of phosphate buffer with fructose (0.1 M) or glucose (0.3 M) at pH = 7.4. The buffer outside the dialysis bag was taken at regular intervals to check the fluorescence emission (excitation wavelength of 495nm). Without monosaccharides in buffer, no fluorescence was observed from the buffer solution.

Methodology for Screening PBOX (qualitative ARS assay) [25, 26, 27]

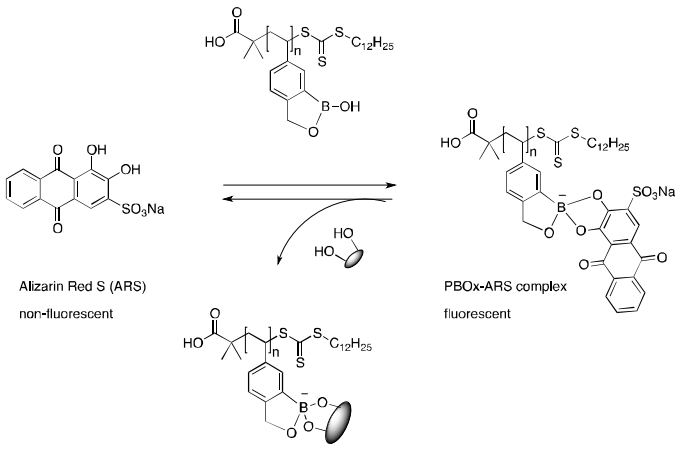

Scheme 2.2 Wang's competitive binding assay of boronic acids with carbohydrates using Alizarin Red S (ARS) as a colorimetric reporter.

Methodology and Examples for *Ka* measurements by ARS method[25, 26, 27]

Equations for association constant determinations.

$1/\Delta I_f = (\Delta K\ p_o I_o K_{eq1})^{-1} /[R] + (\Delta K\ p_o I_o)^{-1}$ (1)

Where ΔK , p_o, I_o are all the parameters of the fluorescence spectrophotometer, R is receptor (PBOx) and I_f is fluorescent intensity

$Q = [I]/[RI] = (I_{RI}- I)/ (I - I_I)$ (2)

Where A is measured absorbance, I_{RI} is intensity of the receptor-indicator (PBOx-ARS) complex, and I_I is intensity of free indicator.

$P = [R_0] - 1/ (Q K_{eq1}) - [I_0]/ (Q+1)$. (3)

R_0 is the total amount of PBOx and I_0 is the total amount of ARS

$[S]/P = (K_{eq1}/K_{eq})Q + 1$ (4)

where [S] is substrate concentration

The equilibrium constant for PBOx – diol complex (K_{eq1}) is obtained by ARS competitive experiments as following the procedure of Wang et al.,[4] 0.144 mM ARS solution was prepared in 0.1 M phosphate solution buffered at pH 7.4. Then, a PBOx was added to give solutions with a range of PBOx concentrations (1.25×10^{-3} - 1.27×10^{-2} M) and fluorescent intensities were measured with excitation wavelength of 468nm and emission wavelength of 572nm. The relationship between fluorescent intensity changes and equilibrium constant can be expressed using (Equation 1). The association constant for the ARS-PBOx (K_{eq1}) is the quotient of the intercept and the slope in a plot of $1/\Delta I_f$ versus 1/[R]. Two experiments were done to measure an average value of K_{eq1}.

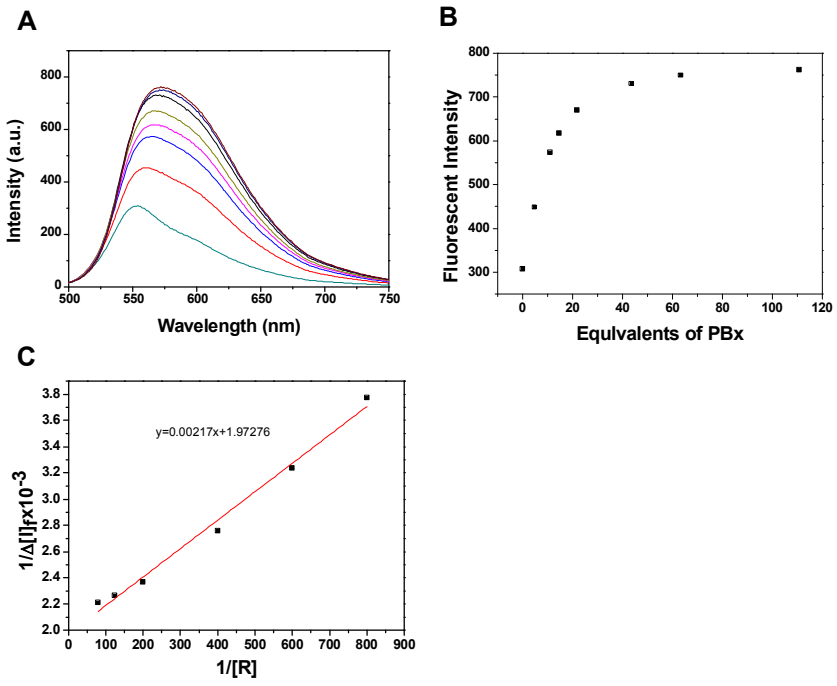

Figure 2.11 ARS (1.145×10^{-4} M) fluorescent profile (λ_{ex}=468 nm, λ_{em}=572 nm) with increasing concentration of ABS-PBOx complex (1.27×10^{-2} M, 5×10^{-3} M, 2.5×10^{-3} M, 1.67×10^{-3} M, 1.25×10^{-3} M, 0 M) (B) Fluorescent intensity increase of ARS (1.145×10^{-4} M) in the presence of PBOx (pH 7.4, 0.1m phosphate buffer). (C) $1/\Delta I_f$ versus 1/[R] for determination of ARS-PBOx (K_{eq1}) in the presense ARS (1.145×10^{-4} M) PBOx (1.25×10^{-3}– 1.27×10^{-2}). K_{eq1} = 909.077

Binding of PBOx with Glucose in the Three-Component Assay. The PBOx and ARS concentration were fixed at 3.1×10^{-3} M and 9.0×10^{-5} M, respectively in a 0.1 M phosphate buffer solution at pH

7.4 (solution A). 5mL of solution A was used to make 2.0 M glucose solution at pH 7.4 (solution B). By mixing the A and B solutions together, a range of glucose concentrations (0.13 – 0. 66 M) was obtained. The K_{eq} is determined by equation 3 and 4

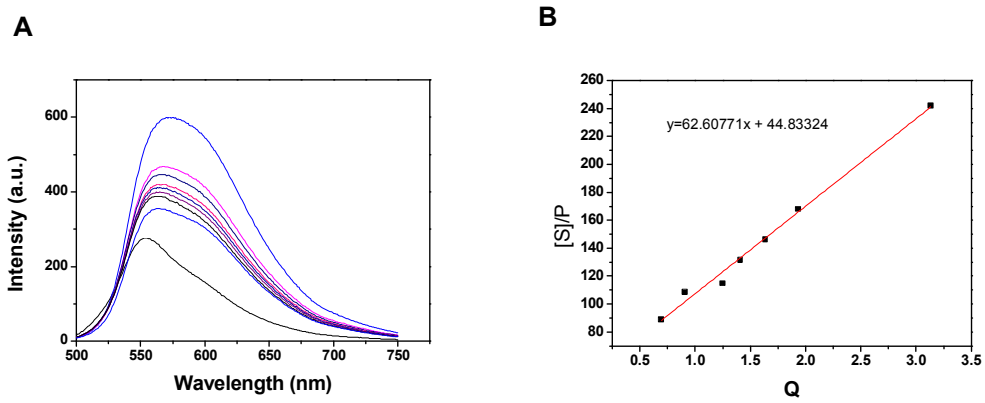

Figure 2.12 (A) ARS fluorescent profile binding of PBOx (3.1 mM) with increasing glucose concentration (0 M, 0.13 M, 0.2 M, 0.25 M, 0.3 M, 0.35 M, 0.42 M 0.66 M, 1.0 M) (B) [S]/P versus Q plot for binding of PBOx (3.1MM) with glucose (0.13-0.66) in the three component with the ARS solution (9×10^{-5} M). K_{eq} = 14.52.

Binding of PBOx with Fructose in the Three-Component Assay. The PBOx and ARS concentration were fixed at 3.1×10^{-3} M and 9.0×10^{-5} M, respectively in a 0.10 M phosphate buffer solution at pH 7.4 (solution A). 5mL of A solution was used to make 2.0 M fructose solution at pH 7.4 (solution B). By mixing A and B solutions together, a range of fructose concentrations (0.00325 – 0.03 M) was obtained. The K_{eq} is determined by equation 3 and 4

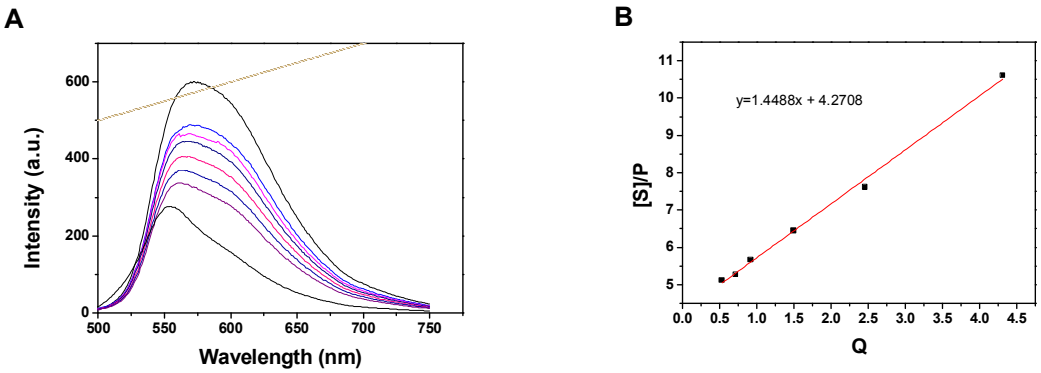

Figure 2.13 (A) ARS fluorescent profile binding of PBOx (3.1 mM) with increasing fructose concentration (0, 0.00325 M, 0.005 M, 0.008 M, 0.0105 M, 0.015 M, 0.02 M, 0.03 M) (B) [S]/P versus Q plot for binding of PBOx (3.1 M) with fructose (0.005–0.03 M) in the three component with the ARS solution (9×10^{-5} M). K_{eq} = 643.3.

References

1. Tanner, P.; Baumann, P.; Enea, R.; Onaca, O.; Palivan, C.; Meier, W. *Acc. Chem. Res.* **2011**, *44*, 1039.

2. Meng, F.; Zhong, Z. *J. Phys. Chem. Lett.* **2011**, *2*, 1533.

3. Brinkhuis, R. P.; Rutjes, F. P. J. T.; van Hest, J. C. M. *Polym. Chem*. **2011**, *2*, 1449.

4. Discher, D. E.; Eisenberg, A. *Science* **2002**, *297*, 967.

5. Meng, F.; Zhong, Z.; Feijen, J. *Biomacromolecules* **2009**, *10*, 197.

6. Li, M.-H.; Keller, P. *Soft Matter* **2009**, *5*, 927.

7. (a) Mabrouk, E.; Cuvelier, D.; Brochard-Wyart, F.; Nassoy, P.; Li, M.-H. *Proc. Natl. Acad. Sci. U.S.A.* **2009**, *106*, 7294. (b) Yu, S.; Azzam T.; Roulier, I.; Eisenberg, A. *J. Am. Chem. Soc.* **2009**, *131*, 10557. (c) Ahmed, F.; Pakunlu, R. I.; Brannan, A.; Bates, F.; Minko, T.; Discher, D. E. J. *Controlled Release* **2006**, *116*, 150. (d) Bellomo, E. G.; Wyrsta, M. D.; Pakstis, L.; Pochan, D. J.; Deming, T. J. *Nat. Mater.* **2004**, *3*, 244. (e) Robbins, G. P.; Jimbo, M.; Swift, J.; Therien, M. J.; Hammer, D. A.; Dmochowski, I. J. *J. Am. Chem. Soc.* **2009**, *131*, 3872.

8. Kim, K. T.; Meeuwissen, S. A.; Nolte, R. J. M.; van Hest, J. C. M. *Nanoscale* **2010**, *2*, 844.

9. Nishiyabu, R.; Kubo, Y.; James, T. D.; Fossey, *J. S. Chem. Commun*. **2011**, *47*, 1106.

10. (a) Cambre, J. N.; Sumerlin, B. S. *Polymer* **2011**, *52*, 4631. (b) Cheng, F.; Jäkle, F. *Polym. Chem.* **2011**, *2*, 2122. (c) Jäkle, F. *Chem. Rev*. **2010**, *110*, 3985. (d) Kanekiyo, Y.; Sano, M.; Iguchi, R.; Shinkai, S. *J. Polym. Sci., Part A: Polym. Chem.* **2000**, *38*, 1302.

11. (a) Kataoka, K.; Miyazaki, H.; Bunya, M.; Okano, T.; Sakurai, Y. *J. Am. Chem. Soc*. **1998**, *120*, 12694. (b) Matsumoto, A.; Yoshida, R.; Kataoka, K. *Biomacromolecules* **2004**, *5*, 1038. (c) Matsumoto, A.; Yamamoto, K.; Yoshida, R.; Kataoka, K.; Aoyagi, T.; Miyahara, Y. *Chem. Commun.* **2010**, *46*, 2203.

12. (a) Cambre, J. N.; Roy, D.; Gondi, S. R.; Sumerlin, B. S. *J. Am. Chem. Soc.* **2007**, *129*, 10348. (b) Roy, D.; Cambre, J. N.; Sumerlin, B. S. *Chem. Commun*. **2008**, 2477. (c) Kim, K. T.; Cornelissen, J. J. L. M.; Nolte, R. J. M.; van Hest, J. C. M. *Adv. Mater.* **2009**, *21*, 2787. (d) Bapat, A. P.; Roy, D.; Ray, J. G.; Savin, D. A.; Sumerlin, B. S. *J. Am. Chem. Soc*. **2011**,

133, 19832. (e) Sumerlin, B. S.; Camber, J. N.; Roy, D. U.S. Pat. Appl. US **2010**/0029545 A1, 2010.

13. Wu, Q.; Wang, L.; Yu, H.; Wang, J.; Chen, Z. *Chem. Rev.* **2011**, *111*, 7855.

14. Wulff, G. *Pure Appl. Chem*. **1982**, *54*, 2093.

15. Kim, K. T.; Cornelissen, J. J. L. M.; Nolte, R. J. M.; van Hest, J. C. M. *J. Am. Chem. Soc*. **200**9, *131*, 13908.

16. (a) Mulla, H. R.; Agard, N. J.; Basu, A. Bioorg. Med. Chem. Lett. 2004, 14, 25. (b) Matsumoto, A.; Ishii, T.; Nishida, J.; Matsumoto, H.; Kataoka, K.; Miyahara, Y. *Angew. Chem., Int. Ed.* **2012**, DOI: 10.1002/ anie.201106252. (c) Li, Y.; Xiao, W.; Xiao, K.; Berti, L.; Luo, J.; Tseng, H. P.; Fung, G.; Lam, K. S. *Angew. Chem., Int. Ed*. **2012**, DOI: 10.1002/anie.201107144.

17. (a) Dowlut, M.; Hall, D. G. J. Am. Chem. Soc. 2006, 128, 4226. (b) Bérubé, M.; Dowlut, M.; Hall, D. G. *J. Org. Chem*. **2008**, *73*, 6471. (c) Pal, A.; Bérubé, M.; Hall, D. G. *Angew. Chem., Int. Ed*. **2010**, *49*, 1492.

18. (a) Jay, J. I.; Lai, B. E.; Myszka, D. G.; Mahalingam, A.; Langheinrich, K.; Katz, D. F.; Kiser, P. F. *Mol. Pharmaceutics* **2010**, *7*, 116. (b) Mahalingam, A.; Geonnotti, A. R.; Balzarini, J.; Kiser, P. F. *Mol. Pharmaceutics* **2011**, *8*, 2465.

19. Springsteen, G.; Wang, B. *Chem. Commun.* **2001**, 1608. (b) Springsteen, G.; Wang, B. *Tetrahedron* **2002**, *5*8, 5291.

20. Qin, Y.; Sukul, V.; Pagakos, D.; Cui, C.; Jäkle, F. *Macromolecules* **2005**, *38*, 8987.

21. Lai, J. T.; Filla, D.; Shea, R. *Macromolecules* **2002**, *35*, 6754.

22. Huang, C.-Q.; Pan, C.-Y. *Polymer* **2010**, *51*, 5115.

23. Lai, J.T.; Filla, D.; Shea, R. *Macromolecules* **2002**, *35*, 6754.

24. Huang, C.-Q.; Pan, C. Y. *Polymer* **2010**, *22*, 5115.

25. Dowlut, M.; Hall, D. G. *J. Org. Chem.* **2008**, *73*, 6471.

26. Springsteen, G.; Wang, B. *Tetrahedro*n **2002**, *58*, 5291.

27. Connors, K. A. *Binding Constants, Wiley: New York,* **1987**.

Chapter 3. Glucose-Responsive Disassembly of Polymersomes of Sequence-Specific Boroxole-Containing Block Copolymers under Physiologically Relevant Conditions

3.1 Abstract

Polymers containing organoboronic acids have recently gained interest as sugar-responsive materials owing to the reversible binding of saccharides to boronic acids, which triggers a change in the physical and chemical properties of these polymers, such as their water solubility. In particular, the ability of these polymers to bind glucose has attracted considerable attention because of the promise of these materials for the development of sensors and drug delivery systems for glucose-related human diseases, such as diabetes. We report here a new class of sugar-responsive polymers that are based on a sequence-specific copolymer of styreneboroxole and *N*-functionalized maleimide. The reversible addition-fragmentation and chain transfer (RAFT) polymerization of this pair of monomers ensured that a glucose-receptor alternates with a non-responsive solubilizing group throughout the sugar-responsive polymer chain. Due to the presence of hydrophilic solubilizing groups beween the solubility-switching boroxole moieties in the membrane-forming block, the polymersomes of the block copolymers responded to a lower level of glucose in the medium, resulting in diassembly of the bilayer membrane under a physiologically relevant pH and glucose-level.

3.2 Introduction

Stimuli-responsive polymers alter their physical and chemical properties in response to the external stimuli. These polymers have been highlighted as smart materials as their functions can be regulated in correspondence to the external stimuli, such as temperature, pH, light, and the presence of stimulant molecules.[1-3] Polymers responsive to biomolecules are particularly interesting due to their potential applications such as sensors and drug delivery vehicles.[4] Polymers containing organoboronic acids recognize monosaccharides and saccharides by way of the reversible covalent bond formation between boronic acid and 1,2- and 1,3-diol compounds.[5-7] In particular, the ability of these polymers to bind glucose has attracted considerable attention because of the promise these materials hold for the development of sensors and drug delivery systems in the treatment of glucose-related human diseases such as diabetes.[8] Controlled radical polymerization of boronic acid-containing vinyl monomers has greatly improved the synthesis of sugar-responsive block copolymers with a well-defined architecture and molecular weight.[9-12] These block copolymers self-assemble into polymeric nanostructures, such as micelles and vesicles,[13,14] which, along with self-regulating hydrogels containing boronic acids as glucose receptors,[15-17] exhibit great potential as drug delivery vehicles that can regulate drug release in accordance with the glucose level in the medium.

Of our particular interest is the use of polymer vesicles (polymersomes)[18,19] formed by self-assembly of sugar-responsive block copolymers as an insulin delivery vehicle. Insulin encapsulated within the water-filled inner compartment of such vesicles can be released *via* sugar-responsive disassembly of polymersomes only when monosaccharides are abound in the surrounding solution.

For applications including glucose sensors and insulin delivery vehicles, boronic acid adopted in a stimuli-responsive polymer should bind to glucose under physiological pH conditions. Under neutral pH conditions, sugar-bornoate ester hydrolyzes due partly to the bond angle strain around a trivalent B center, which requires a tetrahedral geometry to stablized the boronate ester.[20,21] This can be achieved at neutral pH by adopting electron-withdrawing groups[22,23] or electron-donating auxiliary groups to phenylboronic acids,[24] which lowers the pK_a value of the modified boronic acids. We recently synthesized a new class of monosaccharide-responsive polymers constructed by the reversible addition-fragmentation and chain transfer (RAFT) polymerization of styreneboroxole.[25] Benzoboroxole (*o*-hydroxymethylphenylboronic acid) is capable of binding with 6-membered ring sugars (pyranosides) in aqueous solution at a neutral pH, such as the major isomer of glucose in water.[26–30] The resulting poly(styreneboroxole) (PBOx) and its block copolymers with poly(ethylene glycol) as a hydrophilic block (PEG-*b*-PBOx) exhibited the monosaccharide-triggered change in solubility (from insoluble to soluble) in water at a neutral pH. We demonstrated that these well-defined sugar-responsive block copolymers self-assembled into polymersomes, which showed monosaccharide-triggered disassembly of the bilayer membrane, resulting in release of the encapsulated insulin in phosphate buffer at a neutral pH.

Although our results suggested that these sugar-responsive polymersomes have potential as insulin delivery vehicles in the treatment of diabetes, important challenges still remain to be addressed. Despite the enhanced binding of benzoboroxole to glucose at a neutral pH, the polymersomes of made of PBOx block copolymers only exhibited disassembly in the presence of a high concentration of glucose (> 0.3 M), an order of magnitude higher than the concentration of glucose typically found in hyperglycemia (11–20 mM). We reasoned that the requirement of a high glucose level for disassembly of these polymersomes, in part, originates from the fact that glucose can only reach boroxole moieties *via* slow diffusion, propagating from the outer stratum of the bilayer membrane of the polymersome. Unlike hydrogels, in which most glucose-recepting boronic acid groups are exposed to the aqueous environment, most of the boroxole groups in the polymersomes made of PBOx block copolymers are embedded within the bilayer membrane.

We report a new class of sugar-responsive block polymers that are based on a sequence-specific copolymer of styreneboroxole and *N*-functionalized maleimide. The RAFT copolymerization of this pair of monomers ensured that, in the resulting stimuli-responsive polymer, a glucose receptor boroxole alternates with a non-responsive solubilizing group throughout the polymer chain. Due to

the presence of hydrophilic solubilizing groups between the solubility-switching boroxole moieties in the membrane-forming block, the bilayer membrane of these polymersomes are amenable to diffusion of glucose through the membrane, resulting in disassembly of the polymersome at a lower glucose level, close to the physiologically relevant concentration. Given their low toxicity to cells and compatibility with serum, the polymersomes of our block copolymers may find application as smart insulin delivery vehicles of which the release behavior is regulated by the glucose level in the surrounding medium.

3.3 Result and Discussion

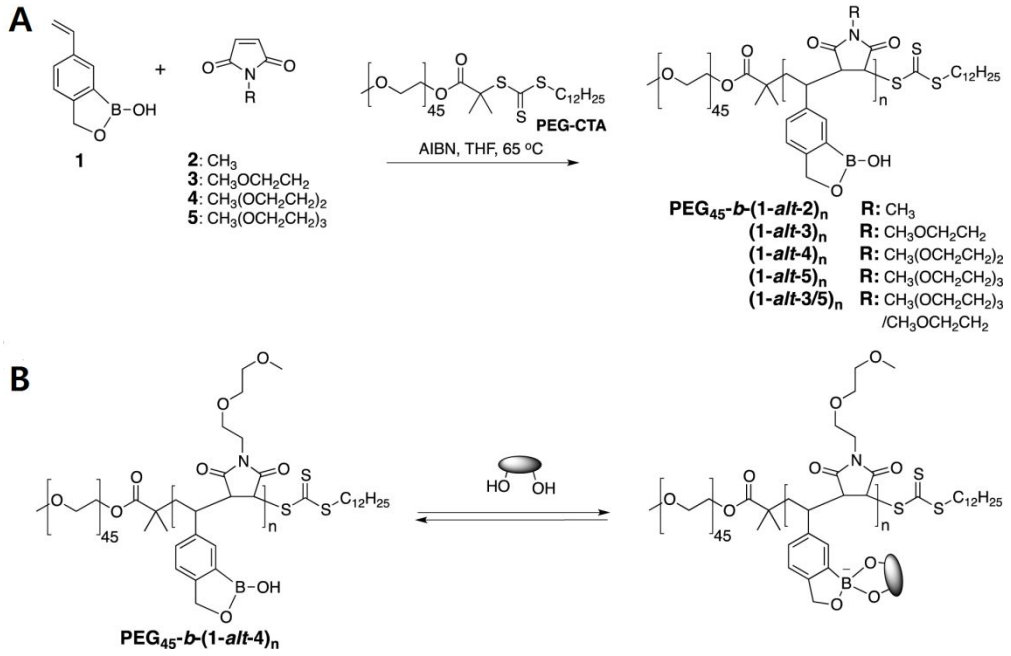

Scheme 3.1 (A) Synthesis of sequence-specific block copolymers of styreneboroxole and *N*-functionalized maleimide by the RAFT polymerization. (B) A schematic representation of sugar-responsive behavior of block copolymers in water.

Synthesis of Sequcnce-Specific Block Copolymers. To implement solubilizing groups in the sugar-responsive backbone in a controllable manner, we adopted an alternating copolymerization of **1** and maleimide **2**−**5** with an *N*-functional group of varying degrees of hydrophilicity to synthesize the glucose-responsive polymer block (Scheme 3.1). The RAFT polymerization of these pairs of monomers with **PEG-CTA**, (M_n(PEG) = 2000 g/mol) yielded block copolymers in which the stimuli-responsive block was composed of an alternating sequence of **1** and maleimide **2**−**5**.[31–33] In a typical procedure, an equimolar mixture of **1** and **4** was used for polymerization with **PEG-CTA** and AIBN

at 65 °C in THF ([**1**]:[**4**]:[AIBN]:[CTA] = 100:100:0.01:1). The progress of polymerization was monitored by ^{1}H NMR until the degree of polymerization (DP_n) of **1** and **4** reached the required value. All polymerization was suspended before the conversion of monomers reached 70 %. ^{1}H NMR analysis of the resulting block copolymers **1-*alt*-4$_n$** indicated equimolar incorporation of **1** and **4** into the stimuli-responsive block, suggesting a strong tendency for alternating polymerization of these monomers (Figure 3.7).[34] The controlled nature of the RAFT polymerization of **1** and **4** was also observed by quenching the polymerization at different reaction times, resulting in a gradual increase in the DP_n of **1** and **4** (Figure 3.1) over the reaction time. GPC experiments of the block copolymers showed a unimodal peak, without any trace of a residual **PEG-CTA**. The molecular weight determined by GPC was compared to the value calculated from ^{1}H NMR integration, which showed a consistent overestimation, as we has previously observed with GPC results of PBOx and their block copolymers (Table 3.1).[25]

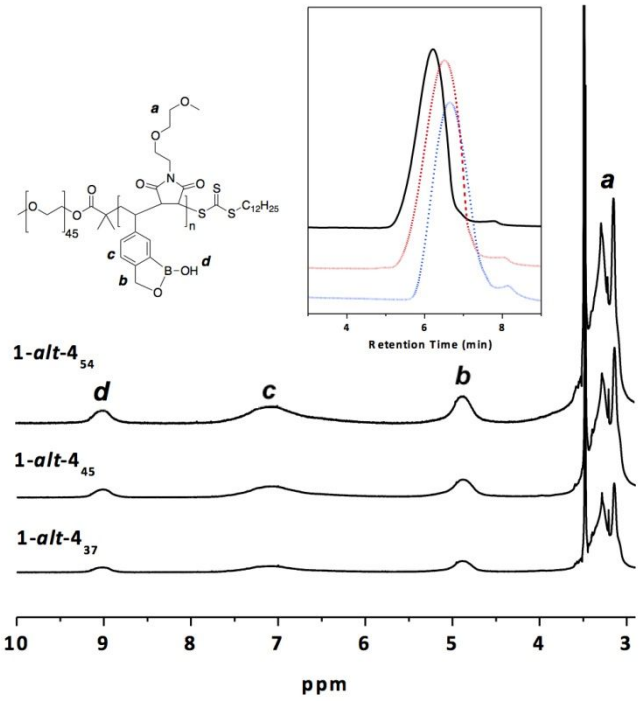

Figure 3.1. ^{1}H NMR (600 MHz, DMSO-d$_6$) spectra of a series of block copolymers **1-*alt*-4$_n$** where the subscript n denotes the calculated degree of polymerization by comparing the integration of a and b by assuming the value of PEG (M_n = 2,000 g/mol, DPn = 45) signal (3.45 ppm). The inset shows GPC traces of **1-*alt*-4$_n$** block copolymers (n = 37 (dotted line), 45 (dashed line), 54 (solid line)).

Table 3.1 Characterization of the block copolymers containing a sequence-specific block.

sample	M_n (g/mol)[a]	DP_n (1-alt-MI)[b]	M_n (g/mol)[c]	PDI[c]	K_a^{fru} (M^{-1})[d]	K_a^{glu} (M^{-1})[d]
1-*alt*-2_{30}	10105	30	**36,700**	**1.24**		
1-*alt*-2_{40}	12806	40	**40,140**	**1.28**		
1-*alt*-2_{50}	15508	50	**46,200**	**1.28**	**541.3**	**13.40**
1-*alt*-3_{30}	11456	30	**38,510**	**1.30**		
1-*alt*-3_{35}	13032	35	**46,900**	**1.32**		
1-*alt*-4_{37}	15293	37	**51,300**	**1.30**		
1-*alt*-4_{45}	18167	45	**50,600**	**1.28**	**526.1**	**13.39**
1-*alt*-4_{54}	21400	54	**71,180**	**1.26**		
1-*alt*-5_{65}	28216	65	**84,330**	**1.35**		
1-*alt*-3/5_{54}	21400	54	**66,440**	**1.30**	**550.1**	**13.20**
1-*alt*-6_{26}	10664	26	**34,710**	**1.25**		

[a] The number average molecular weight determined by ^{1}H NMR integration. [b] The number average degree of polymerization of (1-*alt*-MI)$_n$ determined by ^{1}H NMR integration. [c]The number average molecular weight and polydispersity index obtained by GPC (0.1% DMAC in DMF, 35 °C, 1 mL/min flow rate) using PS standards. [d] Association constants measured by the Wang's method (PBS, 10 % dioxane).

Binding constant of block copolymer with monosaccharides. We measured the binding constant (K_a) of the synthesized boroxole-containing block copolymers to monosaccharides in aqueous solution using the Wang's competitive binding assay (Table 3.1).[20,35] For example, the measured K_a values of the block copolymers **1-*alt*-4_{45}**, as determined using Alizarin Red S (ARS) as a reporter for boroxole-monosaccharide binding, were 13.39 M^{-1} for glucose, and 526.1 M^{-1} for fructose in phosphate buffer (pH 7.4). For **1-*alt*-2_{50}**, K_a was 13.40 M^{-1} for glucose and 541.3 M^{-1} for fructose. These values were close to the binding constants determined for benzoboroxole, and for boroxole-containing polymers and block copolymers.[25,26,36] These results indicated that the alternating sequence of styreneboroxole and maleimide in the polymer chain did not affect the binding between boroxole and monosaccharides.

Self-assembly of block copolymers. Control of the architecture of a block copolymer is crucial for driving its self-assembly process in such that a nanostructure of the desired morphology is achieved. The RAFT alternating copolymerization of **1** and *N*-functionalized maleimides **2**–**5** in the presence of a PEG macro-chain transfer agent allowed us to synthesize amphiphilic block copolymers possessing a sequence-specific sugar-responsive block, of which the degree of polymerization was controlled by virtue of the controlled nature of polymerization. For example, a series of block copolymers **1**-*alt*-**2**$_n$ exhibited a morphological transition from spherical/cylindrical micelles to polymersomes as the DP_n of **1** and **2** in the sugar-responsive block increases from 20 to 50. The block copolymers prepared by the alternating copolymerization of **1** and maleimide having a hydrophilic oligo(ethylene glycol) units as a *N*-functional group (methoxyethyl for **3**, methoxyethoxyethyl for **4**, and methoxyethoxyethoxyethyl for **5**) exhibited a similar morphological transition from micelles to polymersomes with increasing DP_n of a sugar-responsive block (Figure 3.2 and Figure 3.3).

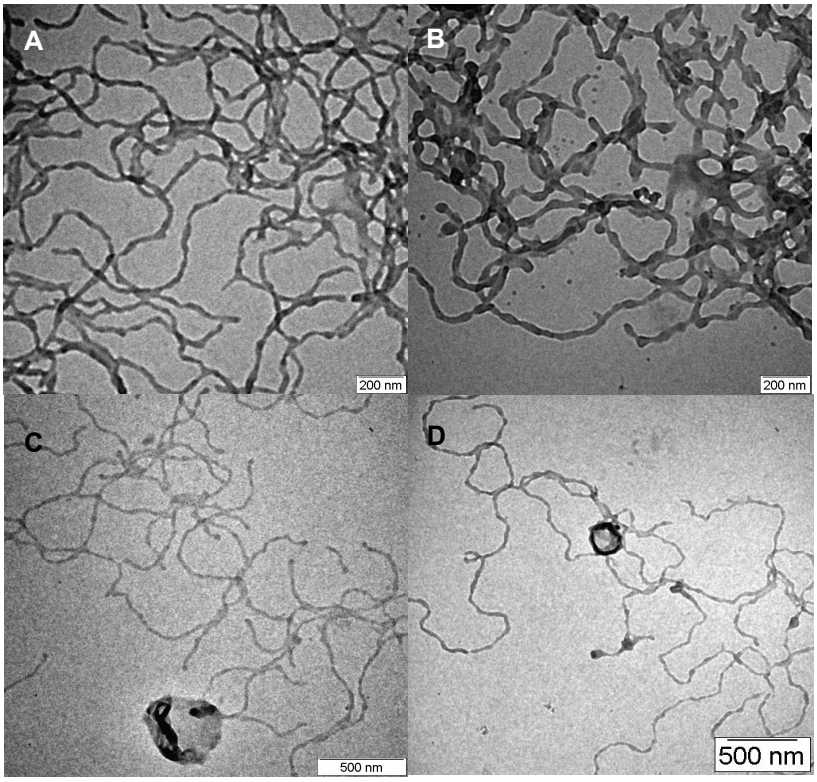

Figure 3.2 TEM images of cylindrical micelles of (A) **1**-*alt*-**2**$_{30}$, (B) **1**-*alt*-**3**$_{30}$, (C) **1**-*alt*-**4**$_{37}$, and (D) **1**-*alt*-**5**$_{50}$

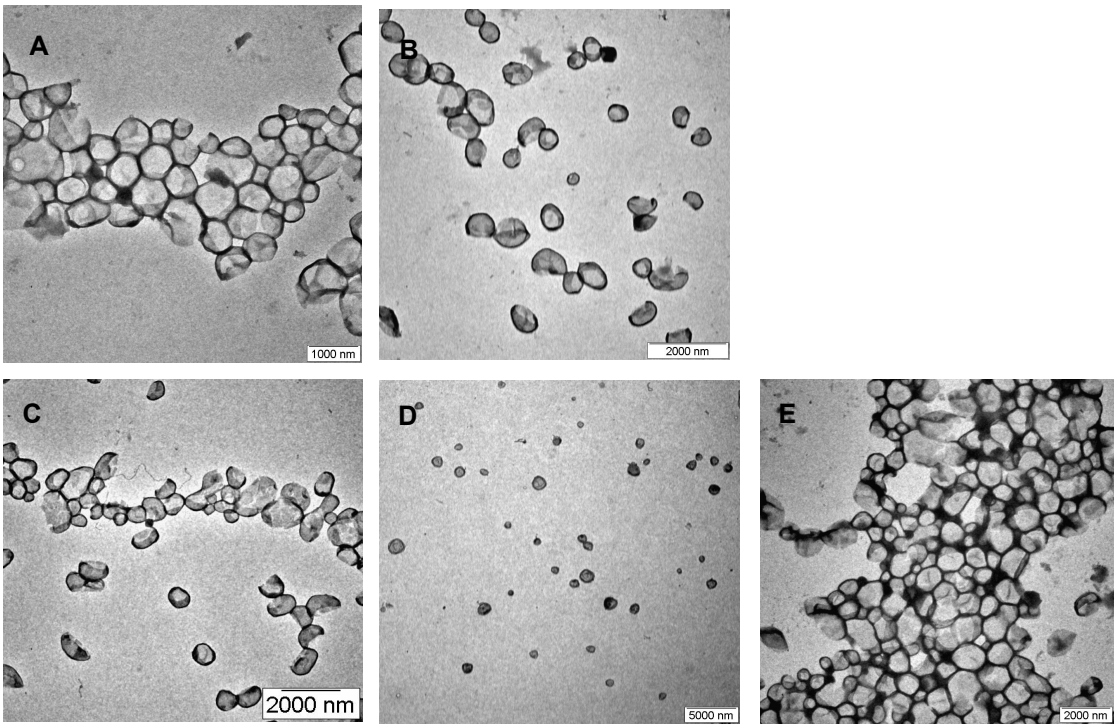

Figure 3.3 TEM images of polymersomes of (A) **1**-*alt*-$\mathbf{2}_{50}$, (B) **1**-*alt*-$\mathbf{3}_{35}$, (C) **1**-*alt*-$\mathbf{4}_{45}$, (D) **1**-*alt*-$\mathbf{5}_{65}$, and (E) **1**-*alt*-**3**/$\mathbf{5}_{54}$.

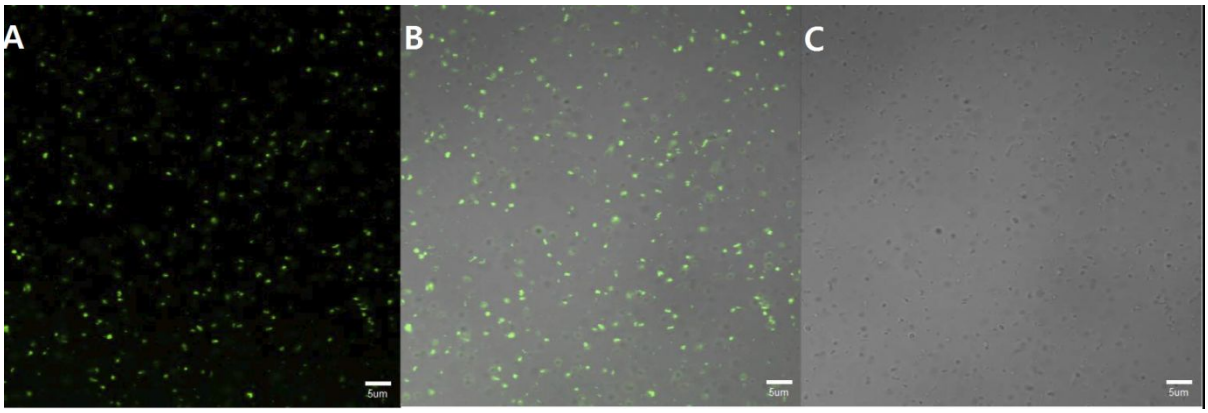

Figure 3.4 Confocal laser fluorescence microscopy of polymersomes of **1**-*alt*-**3**/$\mathbf{5}_{54}$ encapsulating fluorescein-labeled insulin (A) dark field (B) merged (C) bright field images, respectively. scale bars 5 μm.

By observing the morphology of the self-assembled structures on transmission electron microscopy (TEM) and dynamic light scattering (DLS), we identified the optimal DP_n of **1** and maleimide for the formation of polymersomes upon self-assembly for all series of block copolymers

(Figure 3.3). The encapsulation of water-soluble molecules within the polymersomes was demonstrated using fluorescein-labeled insulin (F-insulin) as a guest. For encapsulation, a THF solution of block copolymer **1-*alt*-4$_{45}$** (5 mg/mL) was dispersed in an aqueous solution containing F-insulin (1 mg/mL in phosphate buffer). After dialysis against water and repeated size exclusion chromatography (Sephadex G-50), the polymersome of **1-*alt*-4$_{45}$** encapsulating F-insulin was visualized using a confocal laser fluorescence microscopy (CLFM), which confirmed that the fluorescent guest molecules were well-contained within the polymersomes (Figure 3.4). The purified polymersomes of **1-*alt*-4$_{45}$** encapsulating F-insulin was stable for a period of 4 weeks at ambient temperature, as judged based on DLS and TEM observations.

Glucose-responsive behavior of the polymersomes. The sugar-responsive disassembly of the polymersomes made of block copolymers was studied by measuring the turbidity of the polymersome solution in the presence of glucose in solution by using a UV-Vis spectrometer. When glucose was present in the surrounding solution, disassembly of light-scattering polymersomes, triggered by the binding of boroxole and glucose, resulted in an increase in the optical transmittance measured at 580 nm. We examined the effect of the solubilizing group positioned between boroxole units in the sugar-responsive block by changing the solubilizing group from the least hydrophilic (methyl for **1-*alt*-2$_{40}$**) to the most hydrophilic group (methoxytethoxyethoxyethyl for **1-*alt*-5$_{65}$**). In all cases, no change in optical transmittance was observed for more than 48 h at 36 °C in the absence of glucose in the solution, with the exception of the polymersomes of **1-*alt*-5$_{65}$**, which disassembled completely by 24 h in phosphate buffer lacking glucose. At 0.03 M glucose in buffer (pH 7.6), the polymersome solution of **1-*alt*-2$_{50}$** exhibited virtually no disassembly after 24 h, indicating that the hydrophobic methyl group on maleimide had little effect on increasing the glucose-responsiveness and consequential disassembly of the polymersomes. In contrast, when the solubilizing group was switched to more hydrophilic oligo(ethylene glycol) groups, disassembly of the polymersome solutions of the corresponding block copolymers became noticeably faster. For comparison, the response time (t_R) was defined as the time required for reaching 50 % transmittance at 580 nm at the given glucose concentration. As the number of ethylene glycol units increased from 1 to 2, the t_R decreased from 24.1 h for **1-*alt*-3$_{45}$** to 6.94 h for **1-*alt*-4$_{45}$** (Figure 3.5B).

The most marked effect was observed with the polymersome solution of **1-*alt*-3/5$_{54}$**, the block copolymer that was synthesized using an equimolar mixture of **3** and **5** as a maleimide in pair with **1** to prevent complete dissolution of the block copolymer in buffer without glucose. The polymersome solution of **1-*alt*-3/5$_{54}$** showed a rapid increase of transmittance at 580 nm at a concentration of 0.03 M glucose (t_R = 2.15 h at 36 °C), indicating the enhanced binding between boroxole groups in the sugar-responsive block and glucose (Figure 3.5B). Compared to the glucose-triggered disassembly of **PEG$_{45}$-*b*-PBOx$_{57}$** (1.84 h at 0.5 M glucose in phosphate buffer at pH 7.4), the polymersomes of **1-*alt*-**

3/5$_{54}$ exhibited disassembly at a concentration of glucose an order of magnitude lower that at which the block copolymers with a sugar-responsive block consisting of PBOx showed a glucose-responsive behavior. The turbidity test of the polymersome solution of **1-*alt*-3/5$_{54}$** revealed that the polymersomes respond to a glucose concentration as low as 0.01 M in phosphate buffer (pH 7.6) (Figure 3.5C).

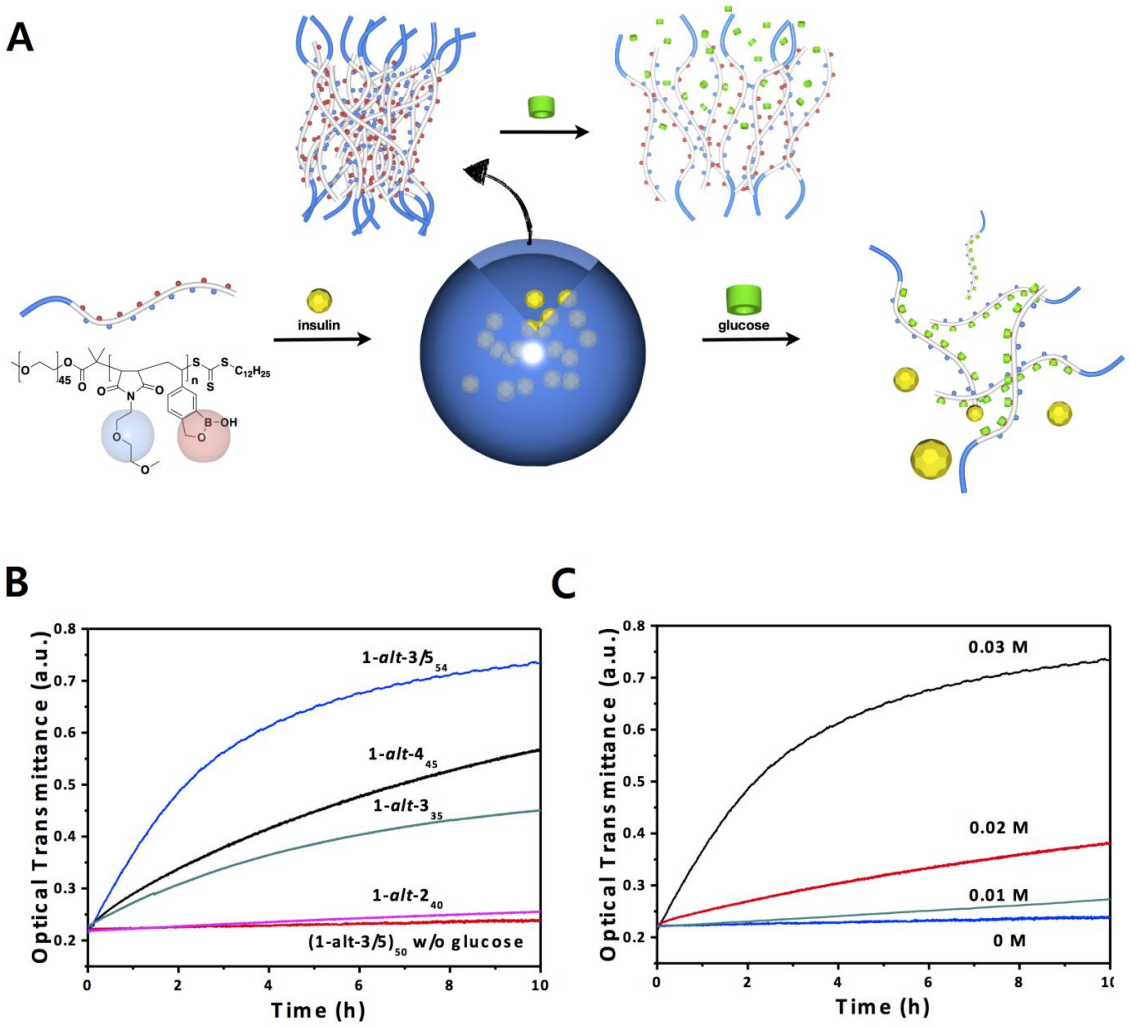

Figure 3.5 (A) A schematic illustration of glucose-triggered disassembly of polymersomes of sugar-responsive block copolymers. (B) Optical transmittance change of polymersome solutions of block copolymers in the presence of 0.03 M glucose (phosphate buffer, pH 7.6, 36 °C). (C) Optical transmittance change of the polymersome solutions of **1-*alt*-3/5$_{54}$** at different concentrations of glucose.

Considering that the measured K_a value of **1-*alt*-3/5$_{54}$** to glucose (13.2 M^{-1}) was nearly identical to the value reported for benzoboroxole and **PEG-*b*-PBOx**, we suspected that this enhanced disassembly of polymersomes arose from the alternating arrangement of a glucose-receptor and a hydrophilic

solubilizing group in the glucose-responsive block. The binding of glucose to boroxole groups surrounded by hydrophilic solubilizing groups may unwind the polymer chains by imparting additional hydrophilicity to the sugar-responsive block. This, in turn, would promote further diffusion of glucose through the bilayer membrane and essentially induce disassembly of the membrane into individual block polymers (Figure 3.5A).

Feasibility of the polymersomes as insulin delivery vehicles in physiologically relevant conditions. To assess the feasibility of using these polymersomes as drug delivery vehicles that can respond to glucose levels under physiologically relevant conditions, we performed the turbidity test using rabbit serum (Sigma). Without glucose in serum, the polymersomes of **PEG$_{45}$-*b*-(1-*alt*-3/5)$_{54}$** showed excellent stability for 24 h at 36 °C; no indications of aggregation or disassembly of the polymersomes were found in the turbidity test and DLS experiments (Figure 3.6A). In the presence of 0.03 M glucose, in contrast, disassembly of the polymersome was observed at a reduced rate (t_R = 7.71 h) compared to the glucose-responsive disassembly in buffer.

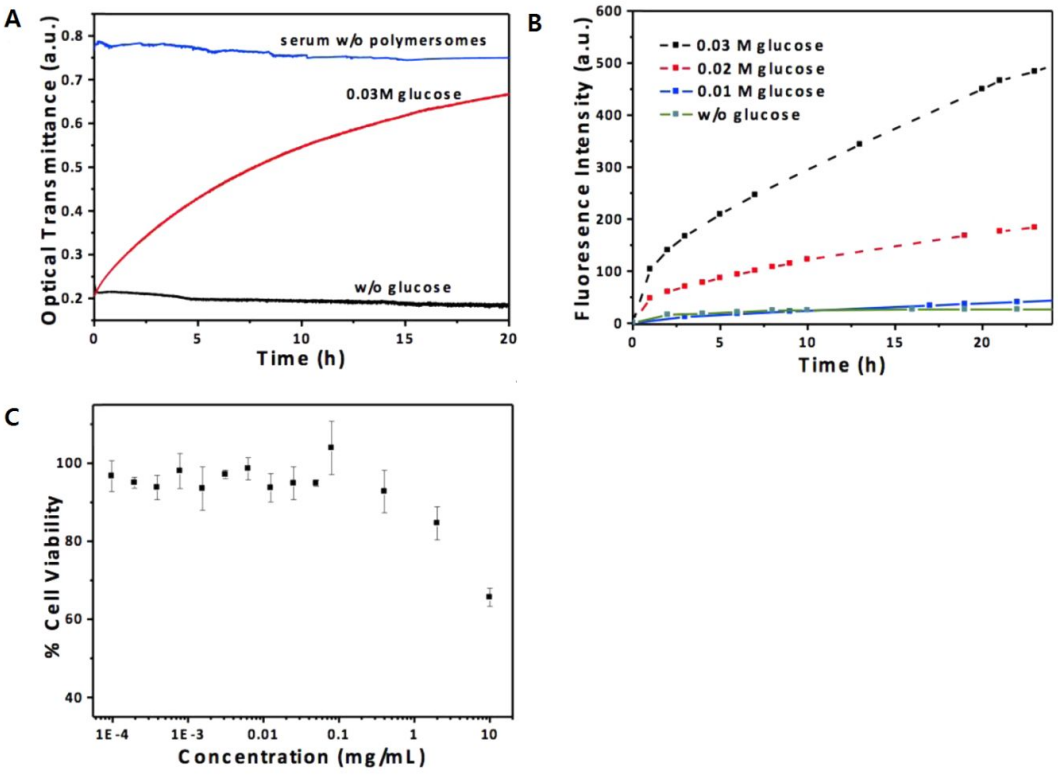

Figure 3.6 (A) Disassembly of the polymersomes of **PEG$_{45}$-*b*-(1-*alt*-3/5)$_{54}$** in serum (rabbit serum, 36 °C) in the presence of 0.03 M glucose. (B) Release profiles of insulin from the polymersomes of **PEG$_{45}$-*b*-(1-*alt*-3/5)$_{54}$** at different concentrations of glucose in phosphate buffer (pH 7.4). (C) Results of the cytotoxicity tests of solutions of **PEG$_{45}$-*b*-(1-*alt*-5)$_{65}$** in HeLa cells after 18 h incubation. N = 3, mean ± SD.

The release of encapsulated guest F-insulin from the polymersomes of **PEG$_{45}$-*b*-(1-*alt*-3/5)$_{54}$** was also investigated at different glucose concentrations in buffer (pH 7.4) (Figure 3.6B). The insulinencapsulating polymersomes of **PEG$_{45}$-*b*-(1-*alt*-3/5)$_{54}$** were contained in a semipermeable membrane (MW cutoff 12 kDa), which was dialyzed against buffer containing the desired concentration of glucose for 24 h. As suggested by the results of the turbidity tests, encapsulated insulin was released from the polymersomes via glucose-triggered disassembly. The rate of release was proportional to the concentration of glucose in the medium as shown in Figure 4b. We also assessed the cytotoxicity of the block copolymer by using **PEG$_{45}$-*b*-(1-*alt*-5)$_{65}$** as a model copolymer due to its solubility in the medium lacking monosaccharides. HeLa cells were incubated with an aqueous solution of the block copolymer at varying concentrations for 18 h. Higher than 90% cell viability was observed with up to 0.3 mg/mL of **PEG$_{45}$-*b*-(1-*alt*-5)$_{65}$**, suggesting that the block copolymer has low cytotoxicity (Figure 3.6C).

3.4 Summary

In summary, we synthesized a new type of glucose-responsive polymers possessing a sequence-specific arrangement of styreneboroxole and *N*-functionalized maleimide by using alternating copolymerization of these monomers under the RAFT condition. Introduction of hydrophilic solubilizing groups, such as oligo(ethylene glycol) at positions adjacent to glucose-binding boroxole groups in the polymer chain, caused the resulting sequence-specific polymer to demonstrate a glucose-responsive solubility change in water at a reduced concentration of glucose (~ 0.02 M) in aqueous solution at neutral pH. The sequence-specific nature of the sugar-responsive polymer was suggested to play a role in enhancing the glucose-responsive behavior at a low glucose-level. Amphiphilic block copolymers constructed using this sequence-specific sugar-responsive polymer block self-assembled into polymersomes in water, which could encapsulate water-soluble molecules, such as fluorescein-labeled insulin, within their inner compartment. The encapsulated insulin was released only when glucose was present in the medium such as neutral pH buffer and serum, *via* the glucose-triggered disassembly of the polymersomes. Given their low cytotoxicity, serum compatibility, and sugar-reponsive behavior at a glucose level close to physiologically relevant conditions, our block copolymers and polymersomes may find application such as smart delivery vehicles for glucose-related diseases such as diabetes.

3.5 Experimental

General Method. All reagents and chemicals were purchased from commercial sources and used as received. All reactions were performed under N_2 unless otherwise noted. NMR spectra were recorded on a Varian VNMRS 600 spectrometer with $CDCl_3$ and DMSO-d_6 as a solvent. THF was distilled over Na/benzophenone before use. Toluene and DMF was distilled over CaH_2. A Cary Eclipse Fluorescence Spectrophotometer was used for all fluorescence studies. The ARS fluorescence intensities were measured with an excitation wavelength of 468nm and an emission wavelength of 572nm. The insulin fluorescent intensities were measured with excitation wavelength of 495 and emission wavelength of 519nm. Transmission electron microscopy (TEM) was performed on a JEOL 1400 microscope at an acceleration voltage of 120 kV. Sample specimens were prepared by placing a drop of the solution on a carbon-coated Cu grid (200 mesh, EM science). After 30 min, the remaining solution on a grid was removed with a filter paper, and the grid was air-dried for 8 h. Dynamic light scattering (DLS) experiments were carried out on a BI-200SM equipped with a diode laser (637 nm, 4 mW). All DLS data were handled on a Dispersion Technology Software (Brookhaven Instruments). Optical density of the solutions was measured on a on a JASCO V-670 UV-Vis spectrophotometer equipped with a thermostat sample holder with a magnetic stirrer. % Transmittance at 580 nm was used to calculate the optical transmittance (O.T) of the solution by the following equation. $O.T = 1 - ((T_{buf} - T_{sol})/T_{buf})$ where T_{buf} was the % transmission of the buffer at 580 nm and T_{sol} was the % transmittance of the solution at the same wavelength. Confocal Laser Scanning Fluorescence Microscopy (CLSM) was performed on a FluoView 1000 Confocal Microscope (Olympus).

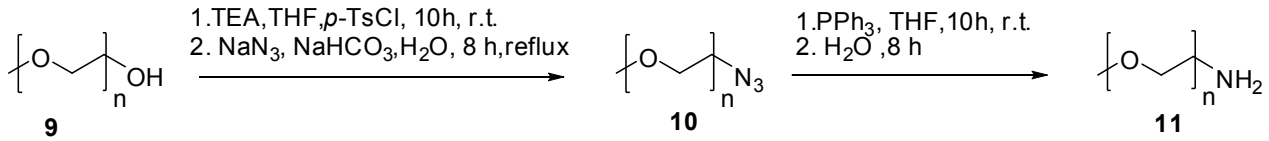

9b: n=1
9c: n=2
9d: n=3

11b: n=1
11c: n=2
11d: n=3

Synthesis of ethylene glycol amine.[37] Ethylene glycol methyl ether **9** (83 mmol) and *p*-toluenesulfonyl chloride (25 g, 127 mmol) were dissolved in dry THF solution (150 mL) and the solution was cooled to 0°C under N_2 in ice/ water. Triethylamine (20.36 mL, 146 mmol) was added dropwise to the reaction flask using a dropping funnel. The mixture was stirred for 10 h. To this mixture, a solution of $NaHCO_3$ (10.0 g, 119 mmol) in water (100 mL) was added, followed by sodium azide (9.5 g, 146 mmol) while stirring. The content was then heated to distill off the THF and refluxed for 8 h. After cooling, the reaction mixture was extracted with ethyl acetate (3 x 70 mL). The organic

layer was washed with brine, dried over anhydrous magnesium sulfate and the organic solvent was evaporated on a rotavap. Colourless oil **10** was obtained.

Compound **10** (55 mmol) and triphenylphosphine (21.77 g, 83 mmol) were dissolved in dry THF solution (300 mL). The reaction mixture was stirred at for 10 h. Then, H_2O (50 mL) was added and the solution further stirred for 8 h under N_2 at room temperature. The THF was evaporated and H_2O (100 mL) was added to the mixture. The reaction mixture was extracted with Toluene (3 x 70 mL). The combined water layer was evaporated on a rotavap.

Monoethylene glycol amine (11b) Colourless oil was obtained. Yield: 4.9 g (72%) ^{1}H NMR (600 MHz, D_2O) δ 3.52 (t, 5.2 Hz, 2H), 3.40 (s, 3H), 2.80 (t, *J* = 5.2 Hz, 3H).

Diethylene glycol amine (11c) Colourless oil was obtained. Yield: 6.9 g (70 %) ^{1}H NMR (600 MHz, D_2O) δ 3.61 (dd, *J* = 5.8, 3.3 Hz, 2H), 3.56 (dd, *J* = 5.5, 3.6 Hz, 2H), 3.52 (t, *J* = 5.2 Hz, 2H), 3.40 (s, 3H), 2.88 (t, *J* = 5.2 Hz, 2H).

Triethylene glycol amine (11d) Colourless oil was obtained. Yield: 11.1 g (82%) ^{1}H NMR (600 MHz, D_2O) δ 3.68 – 3.73 (m, 6H), 3.65 (dd, *J* = 5.6, 3.2 Hz, 2H), 3.60 (t, *J* = 5.4 Hz, 2H), 3.40 (s, 3H), 2.83 (t, *J* = 5.4 Hz, 2H).

Synthesis of maleimide[38]

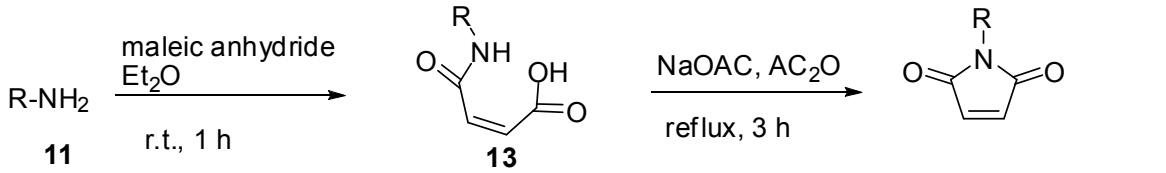

R
11a: CH_3
11b: $CH_3OCH_2CH_2$
11c: $CH_3(OCH_2CH_2)_2$
11d: $CH_3(OCH_2CH_2)_3$
11e: Phenyl

R
2: CH_3
3: $CH_3OCH_2CH_2$
4: $CH_3(OCH_2CH_2)_2$
5: $CH_3(OCH_2CH_2)_3$
6: Phenyl

Methylmaleimide (2). Methylamine hydrochloride **11a** (19.1 g, 280 mmol) was added to a solution of acetic acid (40 ml), maleic anhydride (20.0 g, 200 mmol) and potassium acetate (30.0 g, 300 mmol) and the mixture was stirred for 4 h at reflux temperature (110 ^{o}C). The reaction was cooled and quenched with water. The mixture was poured, slowly, on to the chilled saturated sodium bicarbonate solution (100 mL) and the mixture was extracted with diethyether (3 x 70 mL). The organic layer was washed with brine, dried over anhydrous $MgSO_4$ and the organic solvent was evaporated on a rotavap. The crude mixture was filtered through alumium oxide using CH_2Cl_2 as an eluent. A white solid was obtained. Yield: 6.20 g (20%). ^{1}H NMR (600 MHz, $CDCl_3$) δ 6.70 (s, 2H), 3.02 (s, 3H); ^{13}C NMR (150 MHz, $CDCl_3$) δ = 170.9, 133.3, 23.8; MS (EI) calcd. for $C_5H_5NO_2$ 111.03; found 110.0926.

Monoethylene glycol maleimide (3). Monoethylene glycol amine **11b** (10.0 g, 133 mmol) in 20 mL

Et_2O was added dropwise to maleic anhydride (14.36g, 146 mmol) in 100 mL Et_2O. The reaction mixture was stirred at room temperature for 1h. The solid (monoethylene glycol maleamic acid) precipitated out of the reaction mixture was filtered off. The monoethylene glycol maleamic acid was dissolved in 150 mL of acetic anhydride and 1.2 g of sodium acetate was added to this solution. The mixture was then, refluxed for 2 h with stirring. The reaction was cooled and quenched with water; then, aqueous solution was extracted with Et_2O (3 x 100 mL) and washed with brine. The organic layer was collected and dried with anhydrous $MgSO_4$. After removing the solvent on a rotavap, the crude mixture was purified by silica gel column chromatography (hexane/ethyl acetate 5: 1 v/v). A white crystalline solid was obtained. Yield 16.09 g (78%). ^{1}H NMR (600 MHz, $CDCl_3$) δ 6.70 (s, 2H), 3.72 (t, J = 5.6 Hz, 2H), 3.53 (t, J = 5.6 Hz, 2H), 3.32 (s, 3H). ^{13}C NMR (150 MHz, $CDCl_3$) δ = 170.8, 134.3, 69.45, 58.8, 37.4; MS (ESI) calcd. for $C_7H_9NO_3$ [M + Na^+ + Methanol] 209.06; found 209.725.

Diethylene glycol maleimide (4) Diethylene glycol amine **11c** (3.12 g, 26.2 mmol) in 10mL Et_2O was added dropwise to maleic anhydride (2.34 g, 23.9 mmol) in 100 mL Et_2O. The reaction mixture was stirred at room temperature for 1h and then the reaction mixture was extracted with water (3 x 50 mL). The collected aqueous solution was extracted with CH_2Cl_2 (3 x 50 mL) and washed with brine. The organic layer was collected and dried with anhydrous $MgSO_4$. The combined organic solution was evaporated on a rotavap. The colourless oil was obtained. The diethylene glycol maleamic acid was added in 100 mL of acetic anhydride and 0.8 g of sodium acetate was added. The mixture was then, refluxed for 2 h with stirring. The reaction was cooled and quenched with water; then, aqueous solution was extracted with Et_2O (3 x 100 mL) and washed with brine. The organic layer was collected and dried with anhydrous $MgSO_4$. After removing the solvent on a rotavap, the crude mixture was purified by silica gel column chromatography (hexane/ethyl acetate 3:1 v/v). Colourless oil was obtained. Yield 1.67 g (35%). ^{1}H NMR (600 MHz, $CDCl_3$) δ 6.69 (s, 2H), 3.73 (t, J=5.8 Hz 2H), 3.65 (t, J = 5.8 Hz 2H), 3.60 (t, J = 5.8 Hz, 2H), 3.49 (t, J_1 = 5.8 Hz 2H), 3.34 (s, 3H); ^{13}C NMR (150 MHz, $CDCl_3$) δ = 170.7, 134.3, 72.0, 70.0, 67.9, 59.1, 37.1; MS (ESI) calcd. for $C_9H_{13}NO_4$ [M + $Na]^+$ 222.08, [M + Na^+ + Methanol] 254.08; found 221.74, 253.75.

Triethylene glycol maleimide (5) Triethylene glycol amine **11d** (4.2 g, 26.2 mmol) in 10 mL Et_2O was added dropwise to maleic anhydride (2.34 g, 23.9 mmol) in 100mL Et_2O. The reaction mixture was stirred at room temperature for 1h and then the reaction mixture was extracted with water (3 x 50 mL). The collected aqueous solution was extracted with CH_2Cl_2 (3 x 50 mL) and washed with brine. The organic layer was collected and dried with anhydrous $MgSO_4$. The combined organic solution was evaporated on a rotavap. The colourless oil was obtained. The diethylene glycol maleamic acid was added in 100 mL of acetic anhydride and 0.8 g of sodium acetate was added. The mixture was then, refluxed for 2 h with stirring. The reaction was cooled and quenched with water; then, aqueous solution was extracted with Et_2O (3 x 100 mL) and washed with brine. The organic layer was

collected and dried with anhydrous $MgSO_4$. After removing the solvent on a rotavap, the crude mixture was purified by silica gel column chromatography (hexane/ethyl acetate 2:1 v/v). Colourless oil was obtained. Yield 1.86 g (32%). ^{1}H NMR (600 MHz, $CDCl_3$) δ 6.68 (s, 2H), 3.70 (t, *J*=5.8 Hz 2H), 3.59 (m, 8H), 3.50 (t, *J* = 5.8 Hz, 2H), 3.35 (s, 3H); ^{13}C NMR (150 MHz, $CDCl_3$) δ = 170.77, 134.3, 72.1, 70.7, 70.7, 70.2, 68.0, 59.2, 37.3; MS (ESI) calcd. for $C_{11}H_{17}NO_5$ $[M + Na]^+$ 266.11, $[M + Na^+ + Methanol]$ 298.11; found 265.83 , 297.80.

Phenylmaleimide (6) Aniline (6.04g, 63.5 mmol) in 10 mL $CHCl_3$ was added dropwise to maleic anhydride (5.66g, 57.7 mmol) in 65 mL $CHCl_3$. The reaction mixture was stirred at room temperature for 1h. The solid (phenylmaleamic acid) precipitated out of the reaction mixture was filtered off. The phenylmaleamic acid was dissolved in 125 mL acetic anhydride and 1g of sodium acetate was added. The mixture was then, refluxed for 2 h with stirring. The reaction was cooled and quenched with water; then, aqueous solution was extracted with Et_2O (3 x 100 mL) and washed with brine. The organic layer was collected and dried with anhydrous $MgSO_4$. After removing the solvent on a rotavap, the crude mixture was purified by silica gel column chromatography (hexane:ethyl acetate = 9:1). A yellow solid was obtained. Yield 8.29 g (83 %). ^{1}H NMR (600 MHz, $CDCl_3$) δ 7.44 (t, *J* = 7.5 Hz 2H), 7.34 (t, *J* = 7.5 Hz, 1H), 7.31 (d, *J* = 7.5 Hz, 2H) 6.81 (s, 2H); ^{13}C NMR (150 MHz, $CDCl_3$) δ = 169.3, 134.3, 131.3, 129.3, 128.1, 126.2; MS (EI) calcd. for $C_{10}H_7NO_2$ 173.05; found 172.94.

Synthesis of vinyl boroxole (1) [22] Vinyl boroxole was synthesized by the literature method.

Synthesis of 2-(Dodecylthiocarbonothioylthio)-2-methylpropanoic acid (TC)[39] TC was purchased from Aldrich and also synthesized by the literature method.

Synthesis of TC-terminated poly(ethylene glycol) (PEG-CTA)[40] TC (7.2 g, 20 mmol) and oxalyl chloride (8.6 mL, 100mmol) were added into 40mL dry CH_2Cl_2 and stirred at room temperature until gas evolution stopped. Excess reagents were then removed under vacuum, and the residue was redissolved in 80 mL dry CH_2Cl_2, followed by addition of methoxy poly(ethylene glycol) (Mn = 2000 g/mol) (8 g, 4 mmol in 100mL dry CH_2Cl_2). The reaction was stirred for 24 h at room temperature and the mixture was concentrated before precipitation from an excess of cold Et_2O. The crude polymer obtained by filtration was purified by redisolving in CH_2Cl_2, precipitated in Et_2O, and dried under vacuum overnight. Yellow powder was obtained. ^{1}H NMR (600 MHz, $CDCl_3$) δ 4.25 (t, 2H), 3.64(m, 178H), 3.38 (s, 3H), 3.26 (t, 2H), 1.70 (s, 6H), 1.23-1.40 (m, 20H), 0.88 (t, 3H).

RAFT Polymerization of 4-vinylboroxole and maleimide.

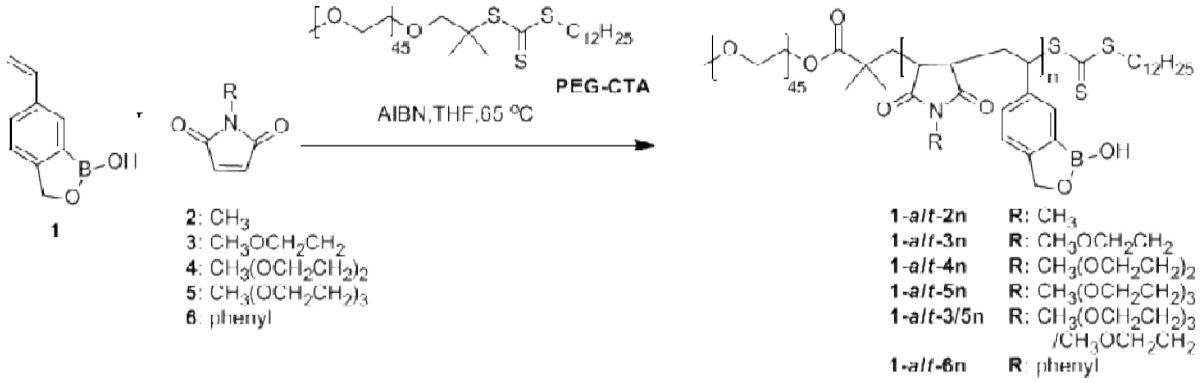

Synthesis of block copolymers PEG-*b*-P(BOx-*alt*-MI) Styreneboroxole **1** (100 mg, 0.625 mmol), maleimide (**2-5**) (0.625 mmol) and **PEG-CTA** (12.5 mg, 6.25 x 10^{-3} mmol) were charged in a Schlenk tube with a magnetic stir bar. This tube was vacuumed and charged with N_2 three times. To this mixture was added 5 mL of dry THF. The solution was degassed by bubbling N_2 for 15 min. A THF solution of AIBN (0.10 mg, 6.25 x 10^{-4} mmol in 0.10 mL) was added at once to this solution, which, then, was immersed into a preheated oil bath (65 °C). The Schlenk tube was sealed, and the polymerization was performed at 65 °C. After polymerization, the reaction mixture was exposed to air and immersed in an ice-water bath. The solution was precipitated into cold diethyl ether. The precipitates were collected by filtration, which were washed profusely with CH_2Cl_2 and dried in vacuum.

Synthesis of block copolymers PEG-*b*-P(BOx-*alt*-3/5)$_n$ Styreneboroxole **1** (100 mg, 0.625 mmol), monoethylene glycol maleimide **3** (48.28 mg, 0.312 mmol), triethylene glycol maleimide **5** (75.9 mg, 0.312 mmol) and **PEG-CTA** (12.5 mg, 6.25 x 10^{-3} mmol) were charged in a Schlenk tube with a magnetic stir bar. This tube was vacuumed and charged with N_2 three times. To this mixture was added 5 mL of dry THF. The solution was degassed by bubbling N_2 for 15 min. A THF solution of AIBN (0.10 mg, 6.25 x 10^{-4} mmol in 0.10 mL) was added at once to this solution, which, then, was immersed into a preheated oil bath (65 °C). The Schlenk tube was sealed, and the polymerization was performed at 65 °C. After polymerization, the reaction mixture was exposed to air and immersed in the ice-water bath. The solution was precipitated into cold diethyl ether. The precipitates were collected by filtration, which were washed profusely with CH_2Cl_2 and dried in vacuum.

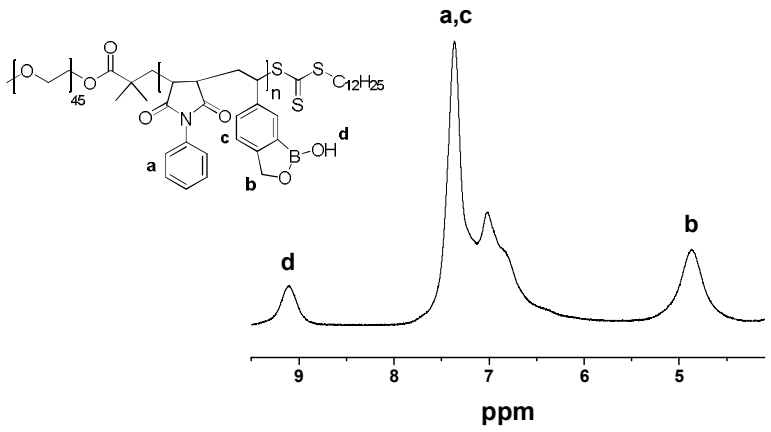

Figure 3.7 Integration of the aromatic sign **a, c** of **1-*alt*-6$_{26}$** and integration of the benzyl signal **b** of the **PBOx** (4.8 ppm) approximately showed 8 : 2 even though Phenyl maleimide was added more than 2 times. This result indicates that this polymer block is composed of the alternating sequence.

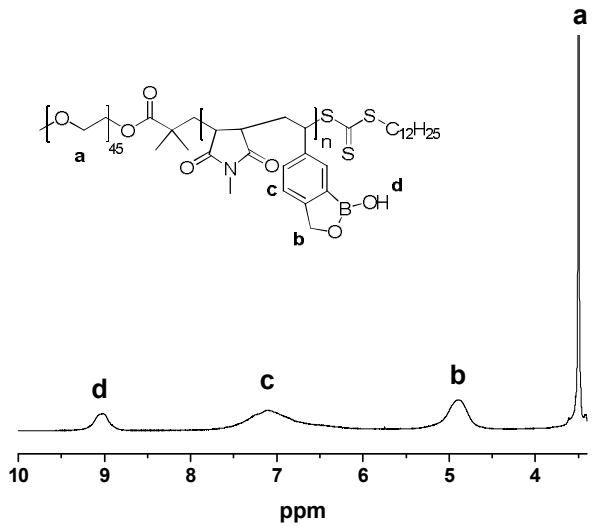

Figure 3.8 ^{1}H NMR (600 MHz, DMSO-d$_6$) spectrum **1-*alt*-2$_n$**. The degree of polymerization of the **1-*alt*-2$_n$** block was calculated by comparing the integration of the benzyl signal **b** of the PBOx (4.8 ppm) and the methylene signals **a** of the PEG (3.6 ppm).

Preparation of Micelle and Polymersome Solutions. Doubly distilled water (MilliQ, 18.1 MΩ) was used throughout the experiments. A typical procedure is described: 1-*alt*-MI_n (10 mg) was dissolved in THF (2 mL) in a 15 mL capped vial with a magnetic stirrer. The solution was stirred for 3 h at room temperature. A syringe pump was calibrated to deliver water at a speed of 2 mL/h. The vial cap was replaced by a rubber septum. 4 mL of water was added to the organic solution with vigorous stirring (850 rpm) by a syringe pump with a 5 mL syringe equipped with a steel needle. The remaining solution was subjected to dialysis (SpectraPor, molecular weight cut-off: 12,000−14,000 Da) against water for 24 h with a frequent change of water. The resulting suspension was collected from a dialysis bag. The diameter and morphology of polymersomes were studied by dynamic light scattering (DLS) and TEM.

Dynamic light scattering (DLS) experiments

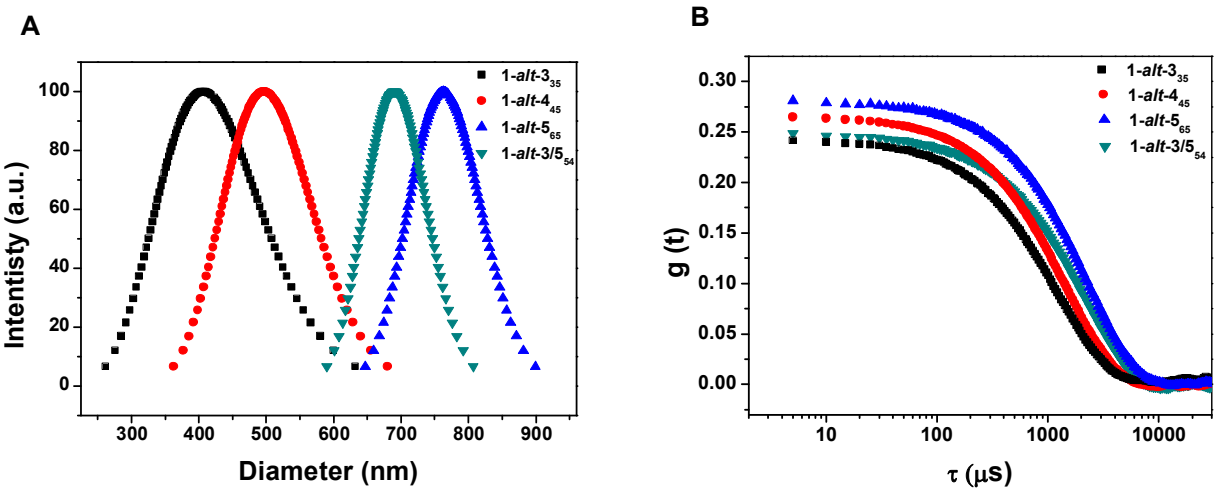

Figure 3.9 (A) Size distribution (B) Autocorrelation functions of polymersomes in water. D_{av} (PDI) for polymersomes: **1-*alt*-3$_{35}$**, 403.4 nm (0.219); **1-*alt*-4$_{45}$**, 484.8 nm (0.207); **1-*alt*-5$_{65}$**, 749.9 nm (0.122); **1-*alt*-3/5$_{54}$**, 657 nm (0.153).

Turbidity Test of Polymersomes. 10 mL of the polymersome solution (phosphate buffer, pH = 7.4) was charged in a 15 mL vial with a magnetic stir bar. To this solution was added glucose (0.1 mmol, 0.2 mmol or 0.3 mmol) at once. After complete dissolution of added sugar, the pH of the solution was readjusted to 7.6 by adding aqueous NaOH (1M). 2 mL of this solution was charged in a quartz cuvette with a magnetic stirrer. The absorbance at 580 nm was measured in every 10 sec with a constant stirring.

Turbidity Test of Polymersomes in serum. 5mL serum (Rabbit serum, Sigma) passed through 0.2μm syringe filter and 5 mL of the polymersome solution (phosphate buffer, pH = 7.4) were charged in a 15 mL vial with a magnetic stir bar. To this solution was added glucose (54 mg, 0.3 mmol) at once. After complete dissolution of added sugar, the pH of the solution was readjusted to 7.4 by adding

aqueous NaOH (1M). 2 mL of this solution was charged in a quartz cuvette with a magnetic stirrer. The absorbance at 580 nm was measured in every 10 sec with a constant stirring

MTT assay. HeLa cells were plated in 96 well plates (7 X 103 cells / well) and incubated in a 37 ^{o}C and 5% CO_2 incubator for 24 hr. The fresh DMEM medium (10% FBS, 5% Antibiotics) was added to the cells and different concentrations of polymer were treated for 18hr. 0.5 mg/mL Thiazolyl blue tetrazolium bromide solution was added to the cells for 4h and then removed the medium. The cells were then collected in 200 μL of DMSO. This 96-well plate was then measured at 595nm with a microplate reader.

Fluoresce in labelling of insulin. The stock solution of insulin was obtained by dissolving 1 mg of insulin (Human insulin, Sigma) in 0.1 mL of 1 % acetic buffer and the working solution of insulin (0.1 mg/mL) was obtained by diluting the stock solution by 100 folds into reaction buffer containing 50 mM NaH_2PO_4, 100 mM NaCl (pH 7.5). The working solution of insulin was incubated with 10 molar equivalents of *N*-hydroxysuccinimidyl ester (NHS) fluorescein at room temperature with vigorous shaking for one and half hours. Reactions were implemented to dialysis with sterile deionized water to remove unreacted NHS-fluorescein overnight.

FITC-labelled Insulin encapsulation in the polymersome of 1-*alt*-3/5$_{54}$. A 1-*alt*-3/5$_{54}$ (10 mg) was dissolved in THF (2 mL) in a 15 mL capped vial with a magnetic stirrer. The solution was stirred for 3 h at room temperature. A syringe pump was calibrated to deliver Fluorescein-labeled Insulin (F-insulin) in phosphate buffer (1.0 mg/mL) a speed of 2 mL/h. The vial cap was replaced by a rubber septum. 4 mL of F-Insulin was added to the organic solution with vigorous stirring (850 rpm) by a syringe pump with a 5 mL syringe equipped with a steel needle. The remaining solution was subjected to dialysis (SpectraPor, molecular weight cut-off: 12,000−14,000 Da) against phosphate buffer for 1 day with a frequent change of phosphate buffer. The resulting suspension was collected from a dialysis bag, and the suspension was then purified by size exclusion column chromatography (Sephadex G-50), which showed two green bands. The first band was collected and combined.

Preparation and Analysis of Laser Confocal Fluorescence Microscopy Samples. The solution of polymersomes encapsulating fluorescein-labelled insulin was transferred onto chamlide (magnetic chamber for 25 mm coverslip) and the images were taken directly. Confocal fluorescence images were acquired with FV1000 laser confocal fluorescence microscopy (Olympus) with the parameters of 10 % laser power (370 HV), 1 Gain and 21 % offset and excitation and emission wavelength of 494 and 518 nm, respectively. The images were viewed and processed with FV1000 viewer software (Olympus)

Release of F-insulin from polymersome of 1-*alt*-3/5$_{54}$. The polymersome sample (2mL) encapsulating fluorescein-labelled insulin was subjected to a dialysis bag (SpectraPor, molecular weight cut-off: 8,000 Da), which was dialyzed against 100 mL of phosphate buffer with glucose

(0.01~0.03 M) at pH = 7.4. The buffer outside the dialysis bag was taken at regular intervals to check the fluorescence intensity (excitation wavelength of 495nm). Without glucose in buffer, no fluorescence was observed from the buffer solution for a 24 h period.

Methodology and examples for K_{eq} measurements by ARS method

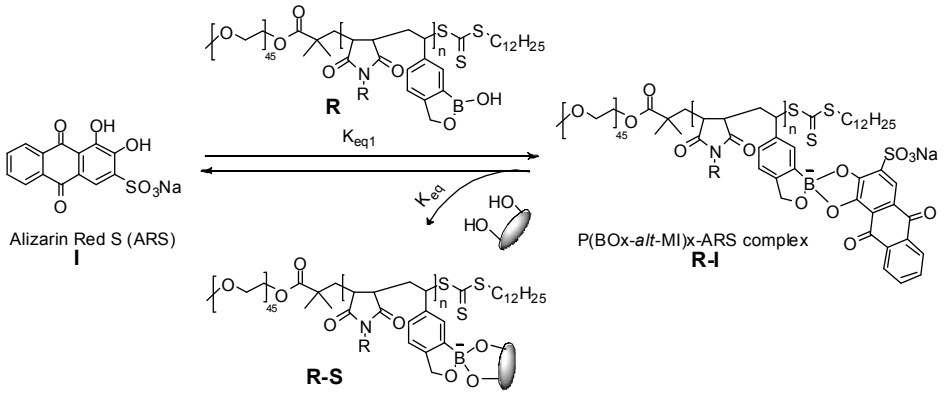

Equations for association constant determinations.

$1/\Delta I_f = (\Delta K\ p_o I_o K_{eq1})^{-1} /[R] + (\Delta K\ p_o I_o)^{-1}$ (1)

Where ΔK , p_o, I_o are all the parameters of the fluorescence spectrophotometer, R is receptor (P(Box-*alt*-MI)) and I_f is fluorescent intensity

$Q = [I]/[RI] = (I_{RI}- I)/ (I - I_I)$ (2)

Where A is measured absorbance, I_{RI} is intensity of the receptor-indicator (P(Box-*alt*-MI) -ARS) complex, and I_I is intensity of free indicator.

$P = [R_0] – 1/ (Q\ K_{eq1}) – [I_0]/ (Q+1)$ (3)

R_0 is the total amount of P(Box-*alt*-MI) and I_0 is the total amount of ARS

$[S]/P = (K_{eq1}/K_{eq})\ Q + 1$ (4)

Where [S] is substrate concentration

The equilibrium constant for P(Box-*alt*-MI) – diol complex (K_{eq1}) is obtained by ARS competitive experiments as following the procedure of Wang et al.,[4] 0.144 mM ARS solution was prepared in 0.1 M phosphate solution buffered at pH 7.4. Then, a 1-*alt*-MI_n was added to give solutions with a range of 1-*alt*-MI_n concentrations (1.25×10^{-3} - 1.27×10^{-2} M) and fluorescent intensities were measured with excitation wavelength of 468nm and emission wavelength of 572nm. The relationship between fluorescent intensity changes and equilibrium constant can be expressed using (Equation 1). The association constant for the ARS- 1-*alt*-MI_n (K_{eq1}) is the quotient of the intercept and the slope in a plot of $1/\Delta I_f$ versus 1/[R]. Two experiments were done to measure an average value of K_{eq1}.

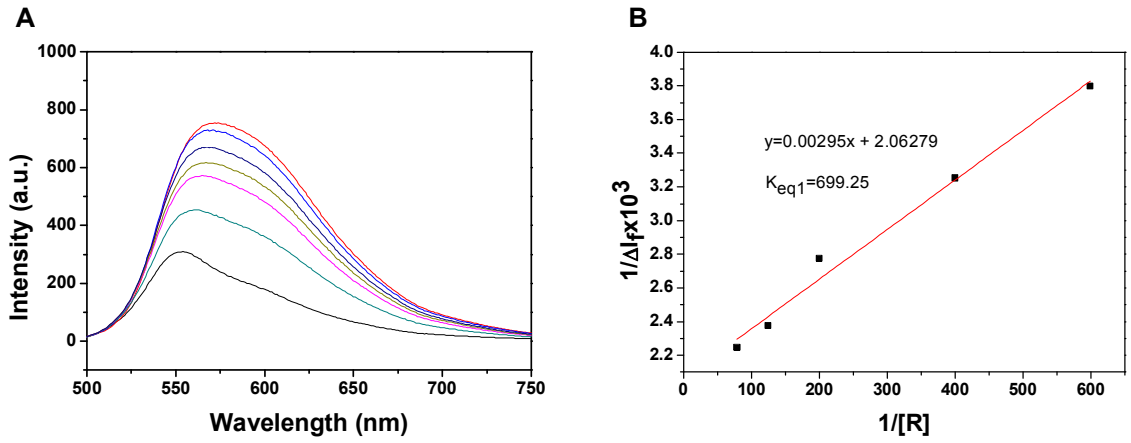

Figure 3.10 (A) ARS (0.144 mM) fluorescent profile (Exc. λ=468 nm, Em. λ=572 nm) with increasing concentration of ABS-1-*alt*-4_{45} complex (1.27×10^{-2} M, 5×10^{-3} M, 2.5×10^{-3} M, 1.67×10^{-3} M, 1.25×10^{-3} M, 0) (B) 1/ΔIf versus 1/[R] for determination of ARS-1-*alt*-4_{45} (K_{eq1}) in the presence ARS (1.145×10^{-4} M) and 1-*alt*-4_{45} (1.25×10^{-3} - 1.27×10^{-2} M). $K_{eq1} = 699.25$

Binding of 1-*alt*-MI_n with glucose in the three-component assay

The P(Box-*alt*-MI) and ARS concentration were fixed at 3.1×10^{-3} M and 9.0×10^{-5} M, respectively in a 0.1 M phosphate buffer solution at pH 7.4 (solution A). 5mL of solution A was used to make 2.0 M glucose solution at pH 7.4 (solution B). By mixing the A and B solutions together, a range of glucose concentrations (0.13 – 1.0 M) was obtained. The K_{eq} is determined by equation 3 and 4

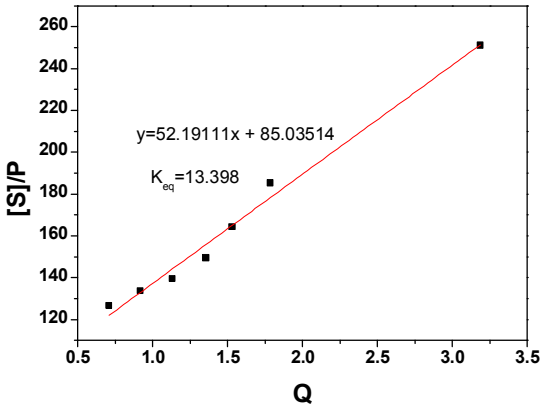

Figure 3.11 [S]/P versus Q plot for binding of 1-*alt*-4_{45} (3.1m M) with glucose (0.13 – 1.0 M) in the three component with the ARS solution (9×10^{-5} M). $K_{eq} = 13.398$

Binding of 1-*alt*-MI_n with fructose in the three-component assay

The 1-*alt*-MI_n and ARS concentration were fixed at 3.1×10^{-3} M and 9.0×10^{-5} M, respectively in a 0.10M phosphate buffer solution at pH 7.4 (solution A). 5mL of A solution was used to make 2.0 M fructose solution at pH 7.4 (solution B). By mixing A and B solutions together, a range of fructose concentrations (0.00325 - 0.03 M) was obtained. The K_{eq} is determined by equation 3 and 4

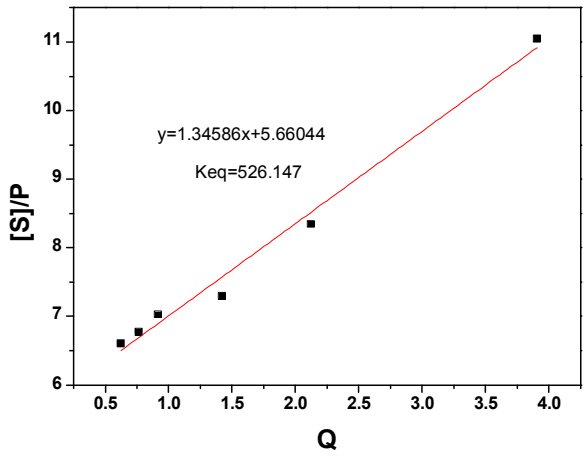

Figure 3.12 [S]/P versus Q plot for binding of 1-*alt*-4_{45} (3.1 mM) with fructose (0.005 - 0.03 M) in the three component with the ARS solution (9×10^{-5} M). K_{eq} = 526.14

References

1. Roy, D.; Cambre, J. N.; Sumerlin, B. S *Prog. Polym. Sci*. **2010**, *35*, 278.
2. Meng, F.; Zhong, Z.; Feijen, J. *Biomacromolecules* **2009**, 10, 197.
3. Li, M.-H.; Keller, P. *Soft Matter* **2009**, *5*, 927.
4. Kim, K. T.; Meeuwissen, S. A.; Nolte, R. J. M.; van Hest, J. C. M. *Nanoscale* **2010**, *2*, 844.
5. Cambre, J. N.; Sumerlin, B. S. *Polymer* **2011,** *52*, 4631.
6. Jäkle, F. *Chem. Rev.* **2010,** *110*, 3985.
7. Cheng, F.; Jäkle, F. *Polym. Chem.* **2011**, *2*, 2122.
8. Wu, Q.; Wang, L.; Yu, H., Wang, J.; Chen, Z. *Chem. Rev.* **2011** *111*, 7855.
9. Qin, Y.; Cheng, G.; Sundararaman, A.; Jäkle, F. *J. Am. Chem. Soc.* **2002**, *124*, 12672.
10. Qin, Y.; Sukul, V.; Pagakos, D.; Cui, C.; Jäkle, F. *Macromolecules* **2005**, *38*, 8987.
11. Cambre, J. N.; Roy, D.; Gondi, S. R.; Sumerlin, B. S. *J. Am. Chem. Soc.* **2007**, *129*, 10348.
12. Vancoillie, G.; Pelz, S.; Holder, E.; Hoogenboom, R. *Polym. Chem.* **2012**, *3*, 1726.
13. Roy, D.; Cambre, J. N.; Sumerlin, B. S. *Chem. Commun.* **2009**, 2106.
14. Kim, K. T.; Cornelissen, J. J. L. M.; Nolte, R. J. M.; van Hest, J. C. M. *Adv. Mater.* **2009**, *21*, 2787.
15. Kataoka, K.; Miyazaki, H.; Bunya, M.; Okano, T.; Sakurai, Y. *J. Am. Chem. Soc.* **1998***, 120*, 12694.
16. Matsumoto, A.; Yamamoto, K.; Yoshida, R.; Kataoka, K.; Aoyagi, T.; Miyahara, Y. *Chem. Commun*. **2010**, *46*, 2203.
17. Matsumoto, A.; Ishii, T.; Nishida, J.; Matsumoto, H.; Kataoka, K.; Miyahara, Y. *Angew. Chem. Int. Ed.* **2012**, *51*, 2124.
18. Discher, B. M. et al., *Science* **1998**, *284*, 1143.
19. Discher, D. E.; Eisenberg, A. *Science* **2002**, *297*, 967.

20. Springsteen, G.; Wang, B. *Tetrahedron* **2002**, *58*, 5291.

21. James, T. D.; Shinkai, S. *Top. Curr. Chem.* **2002**, *218*, 160.

22. Mulla, H. R.; Agard, N. J.; Basu, A. *Bioorg. Med. Chem. Lett.* **2004**, *14*, 25.

23. Roy, D.; Sumerlin, B. S. *ACS Macro Lett.* **2012**, *1*, 529.

24. Kim, K. T.; Cornelissen, J. J. L. M.; Nolte, R. J. M.; van Hest, J. C. M. *J. Am. Chem. Soc.* **2009**, *131*, 13908.

25. Kim, H.; Kang, Y. J.; Kang, S.; Kim, K. T. *J. Am. Chem. Soc.* **2012**, *134*, 4030.

26. Dowlut, M.; Hall, D. G *J. Am. Chem. Soc.* **2006**, *128*, 4226.

27. Bérubé, M.; Dowlut, M.; Hall, D. G. *J. Org. Chem.* **2008**, *73*, 6471.

28. Ellis, G. A.; Palte, M. J.; Raines, R. T. *J. Am. Chem. Soc.* **2012**, *134*, 3631.

29. Sørensen, M. D.; Martins, R.; Hindsgaul, O. *Angew. Chem. Int. Ed.* **2007**, *46*, 2403.

30. Pal, A.; Bérubé, M.; Hall, D. G. *Angew. Chem. Int. Ed.* **2010**, *49*, 1492–1495.

31. Pfeifer, S.; Lutz, J.-F. *J. Am. Chem. Soc*. **2007**, *129*, 9542.

32. Pfeifer, S.; Lutz, J.-F. *Chem. Eur. J.* **2008**, ***14***, 10949.

33. Schmidt, B. V. K. J.; Fechler, N.; Falkenhagen, J.; Lutz, J.-F. *Nature Chem.* **2011**, ***3***, 234.

34. Odian, G. *Principles of polymerization*, 4th Ed., (Wiley, New York, 2004).

35. Springsteen, G.; Wang, B. *Chem. Commun.* **2001**, 1608–1609.

36. Mahalingam, A.; Geonnotti, A. R.; Balzarini, J.; Kiser, P. F. *Mol. Pharmaceutics* **2011**, *8*, 2465.

37. B. C. Mei, K. Susumu, I. L. Medintz, J. B. Delehanty, T. J. Mountziaris, H. Mattoussi, *J. Mater. Chem*. **2008**, *18*, 4949.

38. E. Gaidamaviviute, D. Tauraite, J. Gagilas, A. Laguavinius, Biochimica et *Biophysica Acta* **2010**, 1395.

39. Lai, J.T.; Filla, D.; Shea, R. *Macromolecules* **2002**, *35*, 6754.

40. Huang, C.-Q.; Pan, C. Y. *Polyme*r **2010**, *22*, 5115.